MINERALOGICAL MAGAZINE

JOURNAL OF THE MINERALOGICAL SOCIETY

Vol. 32 March 1961 No. 252

Occurrence of stokesite in Czechoslovakia.

By F. Čech

Dept. of Mineralogy, Charles University, Prague, Czechoslovakia.

[Communicated by the Editor; read 26 January 1961.]

Summary. Stokesite was found in a lithium-bearing pegmatite at Ctidružice near Moravské Budějovice in Western Moravia (Czechoslovakia) in a close association with cryptocrystalline cassiterite. The type of its occurrence is described and its X-ray powder diffraction data given. This represents only the second occurrence of this very rare hydrous silicate of tin and calcium.

THE very rare tin-bearing silicate stokesite, of the formula $CaSnSi_3O_{11}H_4$, was described by Hutchinson (1899, 1900) from Roscommon Cliff, St. Just, Cornwall. At this locality it had been found in the form of a single 1-cm. colourless crystal together with crystals of axinite, in the cavity of a sample. A second occurrence has now been discovered by the present author in Czechoslovakia. It was found as a product of the hydrothermal phase in lithium-bearing pegmatite near Ctidružice in the vicinity of Moravské Budějovice in Western Moravia.

The lithium-bearing pegmatite from Ctidružice forms a body in which, progressing to the centre, the following types of pegmatite may be found: pegmatite of granitoid texture with frequent biotite; pegmatite with black tourmaline and pegmatite of graphic texture; coarser-grained pegmatite composed of larger grains (up to 7 cm.) of potassium feldspar and quartz. Each of the above-named pegmatite types forms an independent zone, the zones passing one into the other gradually. These zones were formed by fractional crystallization of a pegmatite magma. The second stage in the development of the pegmatite represents a sodium replacement unit, which is characterized by abundant occurrence of albite, developed in the form of cleavelandite. Of less frequent occurrence is a lithium replacement unit represented mainly by lepidolite. In addition to common minerals, such as quartz and feldspars, the pegmatite contains the following mineral association: amblygonite (?), apatite,

bertrandite, beryl, biotite, cassiterite, chlorite (alteration product of biotite), columbite-tantalite, hambergite, lepidolite, tourmaline (varieties elbaite and schorl), and zircon (cyrtolite). Pseudomorphs of bertrandite after hambergite described by the present author at an earlier date (1957) are of great interest.

Cassiterite occurs in the pegmatite body in two varieties. Dark brown to brown-black small grains or imperfectly developed crystals of cassiterite of the first variety are usually intergrown in the coarser-grained pegmatite. A similar cassiterite may be encountered quite commonly in lithium-bearing pegmatites in Western Moravia. Toward the end of the entire pegmatite process a new import of SnO_2 material took place

TABLE I. X-ray powder data for stokesite from Ctidružice, Western Moravia, Czechoslovakia. Cu/Ni radiation, 114·59 mm.-diameter camera.

I.	*d.*	*I.*	*d.*	*I.*	*d.*
*8	7·25 Å.	*3	2·23 Å.	*5	1·556 Å.
*6	5·81	*3	2·16	1	1·542
<1	4·95	3	2·13	*3	1·513
1	4·78	*5	2·04	2	1·491
*3	4·54	1	1·992	2b	1·451
*9	3·98	2	1·943	1b	1·427
2	3·76	2	1·910	*2	1·388
*3	3·55	<1	1·879	1	1·373
*2	3·44	*4	1·834	3	1·324
*3	3·04	1	1·812	<1	1·311
*10b	2·88	*3	1·779	<1	1·304
*3	2·70	1	1·755	<1	1·290
2b	2·63	1	1·731	1	1·253
1	2·53	*2	1·714	1	1·234
1	2·47	<1	1·695	*2	1·197
*4	2·39	2b	1·674	2	1·180
<1	2·36	1	1·595		
*3	2·27	<1	1·580		

during the hydrothermal phase. A second variety of cassiterite was formed, which by its appearance and properties strongly reminds one of 'wood-tin'. It is predominantly cryptocrystalline, soft, sometimes finely powdered and resembling a clay mineral. Its colour varies from a pink-grey through light grey to greyish-white. It often forms characteristic pseudomorphs after lepidolite (Čech, 1955).

In spectral analyses of the last-named variety of cassiterite greater amounts of silicon and calcium were found repeatedly (of the order of 0·1% to 1% or more). The silicon content could be ascribed to impurities of quartz, which cassiterite occasionally contains. The increased calcium content was difficult to explain as no calcium-bearing mineral

could be detected either macroscopically or microscopically to accompany cassiterite. X-ray powder diffraction patterns revealed, beside lines of cassiterite, a number of other, mostly very weak reflections (intensities 2 to <1). In table I these reflections are marked with an asterisk. These interferences pointed to the presence of a small admixture of another component, which could not be identified. Only when the paper by Gay and Rickson (1960) appeared recently, containing the X-ray data of stokesite from the original locality in Cornwall, could it be established that all lines of this unidentified component coincided with the principal intense lines of stokesite. On detailed observation of the samples of cryptocrystalline cassiterite pure stokesite could also be discovered, its minute amount, however, being only sufficient for a powder-pattern analysis.

The sample with stokesite represents a heavily albitized pegmatite with relicts of potassium feldspar. There is an abundant admixture of quartz and an accessorial occurrence of green tourmaline (verdelite). In its appearance the stokesite from Ctidružice differs markedly from the sample from Roscommon Cliff. Whereas stokesite from the British locality possessed the habit of a gypsum-like transparent crystal, the Czechoslovak specimen is chalk-white and forms a layer about 1 mm. thick, filling a short fine fissure in cryptocrystalline cassiterite. The cassiterite is very light brown, of earthy appearance and crumbles easily. The stokesite layer was composed of a number of radial-fibrous fine individuals.

The X-ray powder diffraction data of stokesite from Ctidružice are given in table I and compare well with those for the original stokesite, as published by Gay and Rickson (1960).

Samples with cryptocrystalline cassiterite containing a small admixture of stokesite are deposited in the Collection of the Department of Mineralogy, Charles University, Prague, and in the Collection of the Moravian Museum in Brno.

References.

Čech (F.), 1955. Čas. Morav. musea v Brně, vol. 40, p. 81.
—— 1957. Univ. Carolina-Geol., vol. 3, No. 2, p. 129.
Gay (P.) and Rickson (K. O.), 1960. Min. Mag., vol. 32, p. 433.
Hutchinson (A.), 1899. Phil. Mag., ser. 5, vol. 48, p. 480.
—— 1900. Min. Mag., vol. 12, p. 274.

Kennedyite, a new mineral of the pseudobrookite series.

By O. von Knorring, Ph.D., and K. G. Cox, Ph.D.

Research Institute of African Geology, University of Leeds.

[Read 26 January 1961.]

Summary. A new mineral with the approximate composition of $Fe_2MgTi_3O_{10}$ and isostructural with pseudobrookite $Fe_4Ti_2O_{10}$ has been observed in an olivine–augite–alkali-feldspar rock of the Karroo succession from the Mateke Hills area in south-eastern Southern Rhodesia. Chemical analysis and indexed X-ray powder data (a 9·77, b 9·95, c 3·73 Å.) of the mineral are given, and the name kennedyite is proposed. The name karrooite is proposed for the artificial product $MgTi_2O_5$.

THE Mateke Hills area lies in the south-eastern part of Southern Rhodesia and is characterized by several ring-complexes of late-Karroo age, which are emplaced in an extensive trough of Karroo volcanics with generally thin basal sediments. The Karroo rocks rest unconformably on the paragneisses of the Limpopo valley.

The lower part of the Karroo volcanic succession consists mainly of olivine-rich rocks. These are in part extrusive and may be termed in general limburgites, and in part intrusive as sills, dykes, and plugs. The intrusive rocks are fine- to medium-grained and vary in composition from olivine-dolerites to picritic and shonkinitic types.

The specimens containing the new mineral were collected from what is believed to be an extensive sill at the base of the volcanic succession immediately overlying the Cave Sandstone.

Petrographic description. Under the microscope the rock (table I, anal. 1) consists predominantly of broken and abraded olivine phenocrysts from 1 to 5 mm. in length, smaller euhedral or rounded clinopyroxene crystals, often clustered around the margins of the olivines, and rectangular, lath-shaped to fibrous crystals up to 2 mm. in length of the new mineral, set in a ground-mass of an alkali feldspar, which is intergrown with extremely thin apatite needles (fig. 1).

The olivine is partly altered into serpentine along the cracks and contains in addition red-brown patches of another later alteration product. Small grains of magnetite and minute brownish oriented inclusions producing a schiller structure are common. The clinopyroxene, a light

coloured non-pleochroic variety, appears to be free of inclusions and alteration products.

The new mineral is usually opaque, though some of the smaller crystals, particularly along the margins, are commonly translucent and of a dark brown colour. In these, straight extinction has been observed. The mineral is invariably confined to the feldspar matrix, which consists of

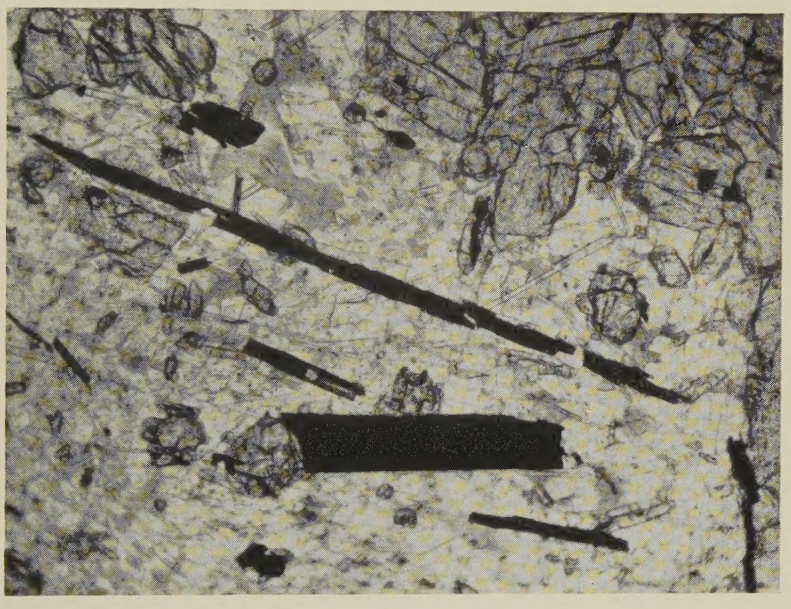

Fig. 1. Kennedyite (opaque) set in a matrix of alkali feldspar with apatite needles. Ordinary light, ×64.

irregular laths without apparent twinning but in which characteristic wavy cracks and undulose extinction have been noted. 2V of the feldspar varies from rather small to moderate; some grains are altered to a greenish sericitic substance; chemical and X-ray data suggest a soda-potash feldspar variety, perhaps an anorthoclase.

An examination of polished sections showed the new mineral in well-defined laths. In some grains marginal patches of secondary hematite were observed and with high magnification (×500) lamellar intergrowths were seen. The lamellae are believed to be exsolved rutile. Pleochroism was not apparent and with crossed nicols only weak steel-grey to purplish-brown anisotropic effects were seen.

Separation of the mineral. The rock contains approximately 3 to 4%

of the new mineral and the separation of this was carried out as follows: the rock was crushed and passed through a 120-mesh sieve. The powder was first repeatedly slimed with water in a large beaker using a little detergent in order to lessen the surface tension. After drying, all magnetic particles were removed with a strong hand magnet and the rest was separated using a Frantz-type magnetic separator, applying a forward slope of 20° and a tilt of 15°. The main fraction containing the new mineral was obtained between 0·6 and 0·8 amps. This fraction was further carefully crushed and slimed and separated with Clerici solution. The mineral was again magnetically separated and a fraction between 0·7 and 0·75 amps. was retained for analysis. Examination under a binocular microscope showed only traces of impurities attached to some of the larger grains, which were removed by hand picking.

Mineralogy and chemistry. The orthorhombic pseudobrookite series is represented by only one naturally occurring mineral, pseudobrookite, Fe_2TiO_5, which was first observed in cavities in an andesite from Aranyer Berg in Transylvania and subsequently described by Koch in 1878 (Dana, 1892). In recent years several artificial compounds with the pseudobrookite structure have been noted in titaniferous slags and others have been synthesized. Indeed, the first synthetic pseudobrookite corresponding to the above formula was found as a sublimate on bricks in a sulphate furnace and reported by Doss as early as 1892.

The chemical analyses of natural pseudobrookites invariably show an excess of titania over the theoretical amount indicated by the formula Fe_2TiO_5 and in addition there is always a small amount of magnesia present. Pauling (1930) made a structural analysis on pseudobrookite crystals from Aranyer Berg and arrived at the same formula, Fe_2TiO_5, as proposed by Doss. He observed, moreover, reflections of rutile in the material examined and the presence of this exsolved mineral phase accounts for the high titania content found in natural pseudobrookites. As for magnesia, no comments were made at the time.

According to Ernst (1943) there is a marked solubility of TiO_2 in pseudobrookite at high temperatures ($>$ 1 500° C.). At lower temperatures the solubility is much reduced and highly titaniferous pseudobrookites should therefore not be common in nature. Among the synthetic compounds with the structure of natural pseudobrookite the following end-members have been recognized: tieilite, Al_2TiO_5; unnamed, $MgTi_2O_5$; anosovite, Ti_2TiO_5; unnamed, $FeTi_2O_5$.

The solid solution series Al_2TiO_5–$MgTi_2O_5$ has been described by Sigurdson and Cole (1949) and the series $MgTi_2O_5$–$FeTi_2O_5$ was noted

by Moore and Sigurdson (1949) in smelting ilmenite ore. Crystals of anosovite, Ti_2TiO_5, have been observed in titaniferous blast furnace slags and studied by Rusakov and Zhdanov (1951) and the Fe_2TiO_5–$FeTi_2O_5$ series has been investigated by Akimoto *et al.* (1957).

In his study on the ore paragenesis of Katzenbuckel in Odenwald, Frenzel (1953) was the first to draw attention to the magnesia content of

TABLE I. Chemical composition of kennedyite and of the kennedyite-bearing rock.

	1.	2.	2*a*.		Norm. of 1.	
SiO_2	46·59	—				
TiO_2	2·83	60·33	Ti	3·27	or	11·7
Al_2O_3	5·89	2·15	Al	0·18	ab	11·5
Fe_2O_3	3·54	28·77	Fe^{3+}	1·56	an	4·7
Cr_2O_3	0·19	0·37	Cr	0·03	di	16·9
FeO	8·31	2·00	Fe^{2+}	0·12	hy	18·1
MnO	0·16	0·07	Mn	0·00	ol	24·2
MgO	21·00	6·45	Mg	0·69	mt	5·1
CaO	5·79	tr.			il	5·3
Na_2O	1·37	—			ap	1·0
K_2O	1·97	—			sal	0·395
H_2O+	1·76	—			fem	
H_2O-	0·10	—				
P_2O_5	0·46	—				
	99·96	100·14				

1. Specimen F 7168/C888. Anal. O. von Knorring.

2. Kennedyite from spec. F 7168/C888, 29 miles ESE. of Nuanetsi, Southern Rhodesia. Anal. O. von Knorring.

2*a*. Atomic ratios to 10 oxygen.

natural pseudobrookites. The pseudobrookite from this locality is associated with hematite, occurs in a natronshonkinite and related rocks, and is considered to have formed by oxidation of original titano-magnetite and ilmenite in connexion with fumarolic or hydrothermal activity. In these pseudobrookites Frenzel has observed variations in the optical properties, which are believed to be related to temperature-controlled changes in the chemical composition of the pseudobrookites.

The chemical composition of the new mineral (table I, anal. 2) is distinctly different from previously analysed pseudobrookites and especially from the accepted composition of pseudobrookite as defined by the formula Fe_2TiO_5. The name kennedyite has been proposed for this new mineral in honour of Professor W. Q. Kennedy. The chemical composition of kennedyite is close to the intermediate member $Fe_2MgTi_3O_{10}$ in the series Fe_2TiO_5–$MgTi_2O_5$. This composition can be deduced from the pseudobrookite formula written as $Fe_4Ti_2O_{10}$ by coupled substitution of MgTi for FeFe.

The chemical analysis also shows considerable amounts of aluminium, ferrous iron, and chromium. A qualitative spectrographic analysis of kennedyite gave the following results: major: Ti, Fe; minor: Mg, Al, Cr; trace: Si, Ca, V, Mn, Ni, Ga, Zr.

TABLE II. X-ray powder data for minerals of the pseudobrookite series. The following cell dimensions were obtained for kennedyite: *a*, 9·77, *b*, 9·95, *c*, 3·73 Å.

	Tieilite Al_2TiO_5		Anosovite Ti_2TiO_5		Kennedyite $Fe_2MgTi_3O_{10}$		Pseudobrookite Fe_2TiO_5		Karrooite $MgTi_2O_5$	
hkl.	*d.*	I/I_1.	*d.*	*I.*	*d.*	*I.*	*d.*	I/I_1.	*d.*	I/I_1.
200	4·71 Å.	47	4·78 Å.	m	4·88 Å.	s	4·902 Å.	45	4·9 Å.	12
220 | 101	3·35	100	3·46	vs	3·485	vs	3·483	100	3·51	100
121					2·855	vw			2·86	9
230	2·65	70	2·70	vs	2·743	s	2·748	80	2·75	60
301	2·36	20	2·42	m	2·450	m	2·454	20	2·45	20
131			2·37	w	2·403	w	2·402	25	2·42	15
240	2·14	31	2·17	m	2·217	w	2·221	11	2·22	15
321	2·11	30	2·14	vw	2·195	w	2·198	15	2·19	20
331	1·897	52	1·93	s	1·970	m	1·971	25	1·967	30
002	1·792	44	1·85	vs	1·865	s	1·862	30	1·876	60
250			1·81	w	1·843	w			1·846	15
022	1·687	28	1·73	m	1·746	w	1·744	15	1·754	15
060	1·606	27	1·65	s	1·661	w	1·663	15	1·665	15
600	1·578	28	1·62	s	1·631	w	1·632	20	1·634	20
	1·519	6	1·58	vw						
	1·484	36	1·54	vs	1·544	m	1·54	35	1·551	30
			1·53	s	1·529	w			1·535	20
	1·449	8	1·49	vw	1·490	vw	1·49	11		
	1·371	14	1·42	s	1·419	vw	1·42	15	1·424	9
			1·37	w	1·370	vw	1·37	9	1·378	8
	1·305	16	1·35	m	1·350	vw			1·358	15
	1·266	11	1·31	vw	1·312	vw	1·31	5	1·318	8
	1·253	11	1·29	m	1·288	vw	1·30	5		
	1·219	9	1·26	m	1·259	vw	1·26	7	1·265	10
			1·24	m	1·240	vw	1·24	5	1·245	10

For the unnamed end-member $MgTi_2O_5$, being one of the major components in the mineral kennedyite, the name karrooite is proposed.

Kennedyite exhibits a tabular to fibrous habit. The colour is normally black, though smaller grains are translucent and are of a dark brown colour. The crystals are striated longitudinally and have a brilliant metallic lustre. The specific gravity determined by suspension in Clerici solution is 4·07, compared with 4·33 for the pseudobrookite from Thomas Range (Dana, 1946). Table II shows the X-ray powder data of kennedyite in relation to the synthetic end-members of the pseudobrookite series. The values for Al_2TiO_5 (tieilite) and $MgTi_2O_5$ (karrooite) are

quoted from Moore and Sigurdson (1949), for anosovite from Zhdanov and Rusakov (1952), and for pseudobrookite from the ASTM X-ray Powder Data File.

In fig. 2 two powder photographs of kennedyite using Fe-$K\alpha$ radiation are shown. The first is on unheated material, the second on ignited (*c.* 1 300° C.) powder. The latter is more clearly defined and shows distinctly an additional line at approximately 4·9 Å., which corresponds to the line at 5·0 Å. given for karrooite. As regards 'impurities' only the strongest line for rutile at approximately 3·2 Å. is discernible.

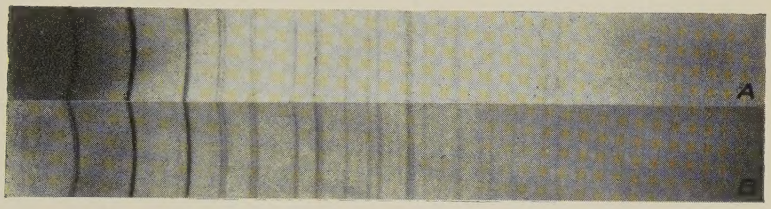

FIG. 2. X-ray powder photographs of kennedyite. 9 cm. camera, Fe-$K\alpha$ radiation. A, unheated material. B, powder heated to 1 300° C. for 5 minutes.

With the knowledge of the above synthetic phases iso-structural with pseudobrookite, the excess titania and additional magnesia reported from natural pseudobrookites can be better understood. The composition of kennedyite gives a further indication of numerous possible diadochic replacements that may take place in the pseudobrookite structure.

The end-members corresponding chemically to pseudobrookite can be assigned the general formula X_2ZO_5 (cf. Zhdanov and Rusakov, loc. cit.). The position of X may be occupied by the following trivalent metals of similar ionic radii (Ahrens' values): Al 0·51 Å., Ti 0·76 Å., V 0·74 Å., Cr 0·63 Å., $Fe^{\cdots}$ 0·64 Å., and Ga 0·62 Å.; Z is represented by quadrivalent Ti 0·68 Å. For the end-members containing divalent ions the formula YZ_2O_5 can be applied. Here Y may be one of the following elements: Mg 0·66 Å., Mn 0·80 Å., $Fe^{\cdot\cdot}$ 0·74 Å., Co 0·72 Å., Ni 0·69 Å., and Zn 0·74 Å. The rock containing kennedyite has a unique chemical composition (table I, anal. 1) and constitutes in itself an interesting petrological problem.

Acknowledgements. The writers wish to express their indebtedness to Professor W. Q. Kennedy, F.R.S., for his interest in the work, to Dr. M. Fleischer of the U.S. Geological Survey for helpful advice, to Miss J. M. Rooke for the spectrographic analysis, and to Mr. W. L. Wilson for X-ray powder photographs.

References.

Akimoto (S.), Nagata (T.), and Katsura (T.), 1957. Nature, vol. 179, p. 37.

Dana (E. S.), 1892. Descriptive Mineralogy, 6th edn. Dana's System of Mineralogy, 7th edn, 1946.

Doss (B.), 1892. Zeits. Kryst. Min., vol. 20, p. 566.

Ernst (Th.), 1943. Zeits. angew. Min., vol. 4, p. 394.

Frenzel (G.), 1953. Heidelberger Beitr. Min. Petr., vol. 3, p. 409.

Moore (C. H., *Jr.*) and Sigurdson (H.), 1949. Metals Transactions, vol. 185, p. 914.

Palache (C.), 1935. Amer. Min., vol. 20, p. 660.

Pauling (L.), 1930. Zeits. Krist., vol. 73, p. 97.

[Rusakov (A. A.) and Zhdanov (G. S.)] Русаков (А.А.) и Жданов (Г.С.) 1951. Доклады Акад. Наук. СССР [Compt. Rend. Acad. Sci. URSS], vol. 77, p. 411.

Sigurdson (H.) and Cole (S. S.), 1949. Metals Transactions, vol. 185, p. 905.

Traube (H.), 1892. Zeits. Kryst. Min., vol. 20, p. 327.

[Zhdanov (G. S.) and Rusakov (A. A.)] Жданов (Г.С.) и Русаков (А.А.) 1952. Доклады Акад. Наук СССР [Compt. Rend. Acad. Sci. URSS], vol. 82, p. 901.

A refinement of the dickite structure and some remarks on polymorphism in kaolin minerals.[1]

By Robert E. Newnham, M.S., Ph.D.

Cavendish Laboratory, Cambridge University
and
Laboratory for Insulation Research, Massachusetts Institute of Technology, Cambridge, Massachusetts, U.S.A.

[Communicated by the Editor; taken as read 26 January 1961.]

Summary. The crystal structure of the clay mineral dickite ($Al_2Si_2H_4O_9$) has been refined to a greater accuracy than that reported in an earlier analysis. Improved lattice parameters are: a 5·150 ± 0·001, b 8·940 ± 0·001, c 14·424 ± 0·002 Å., β 96° 44′ ± 1′. The dickite structure shows several significant distortions from the geometry of the idealized kaolin layer, including deformation and rotation of the silica tetrahedra. The most striking features of the octahedral layer are the extremely short shared edges of 2·37 Å. Although the analysis was not sufficiently accurate to position the hydrogen atoms with certainty, a model consistent with the infra-red absorption spectra is proposed. The stacking sequences of kaolin-layer minerals have been considered with reference to the structural features observed in dickite. There are thirty-six ways of superposing two kaolin layers commensurate with the OH–O bonds found in kaolinite, dickite, and nacrite. The twelve sequences showing the least amount of cation–cation superposition between consecutive kaolin layers can be used to construct two one-layer cells, kaolinite and its mirror image, and twelve two-layer cells, including dickite and nacrite. The distortions of the kaolin layer introduce secondary variations in the interlayer bonding that suggest that dickite and nacrite are the most stable of the kaolin layer structures, since they possess the shortest oxygen–hydroxyl contacts.

THE basic structural unit of the kaolin-clay minerals is the kaolin layer. Its chemical constitution is given by the formula O_3-Si_2-$O_2(OH)$-Al_2-$(OH)_3$, which emphasizes the planar groupings of the structure. Each Si atom is tetrahedrally surrounded by three oxygens in the basal plane and a fourth in the layer above. The latter is shared with two aluminium ions, each of which is octahedrally co-ordinated to two oxygens and four hydroxyl groups, three in the uppermost layer and one coplanar with the apex oxygens. The Si tetrahedra share corners with three other tetrahedra, while each Al octahedron possesses three edges in common with other octahedra. Successive kaolin layers are held to each other only by van der Waals forces and long hydrogen

[1] Supported by the Nuffield Foundation, I.C.I. Ltd., and the U.S. Army Signal Corps, Office of Naval Research, and Air Force.

bonds. Various stacking sequences of the layers lead to several polymorphic structures: kaolinite, dickite, nacrite, and halloysite.

The present investigation is an extension of previous work (Newnham and Brindley, 1956) on the structure of dickite, the best crystallized of the kaolin minerals. A more precise analysis of the structure has been carried out using more experimental data and Fourier projections with less atomic overlap. The discussion of the structure emphasizes the distorted nature of the kaolin layer and its influence on the interlayer bonding and polymorphism problem.

Experimental.

The mineral used came from the Pine Knot colliery in Schuylkill County, Pennsylvania; chemical analysis (Honess and Williams, 1935) has shown this material to be of unusually high purity (46·14 wt. % SiO_2, 39·61 % Al_2O_3, and 13·91 % H_2O, which compares favourably with the theoretical composition: 46·55 % SiO_2, 39·49 % Al_2O_3, and 13·96 % H_2O). The present refinement was carried out on a small, plate-like specimen of dimensions $0{\cdot}20\times0{\cdot}08\times0{\cdot}04$ mm.

The lattice parameters of the dickite unit cell were redetermined from oscillation photographs taken about the a and b axes. The measurements were made on a modified Unicam oscillation camera (Farquhar and Lipson, 1946), in which the photographic film is mounted in the van Arkel position. Zero-layer-line reflections with θ near 90 degrees were measured using Cu-$K\alpha_1$ (λ = 1·54051 Å.) and Cu-$K\alpha_2$ (λ = 1·54433 Å.) radiation, and graphical extrapolation was used to eliminate the major systematic errors. A discussion of the method and the appropriate extrapolation formulae have been given by Weisz, Cochran, and Cole (1949). The results of the final graphical extrapolations are:

a 5·150±0·001, b 8·940±0·001, c 14·424±0·002 Å.

β 96° 44′±1′, V 659·6±0·3 Å^3., d_{002} 7·162±0·001 Å.

The axial ratio $a/b = 0{\cdot}5761\pm0{\cdot}0002$ differs by only 0·22 % from the 'ideal' ratio of $1/\sqrt{3}$. The space group of dickite is C_s^4—Cc with $4[Al_2Si_2O_5(OH)_4]$ per unit cell. The cell contains two kaolin layers related to one another by a c-glide symmetry plane and a stacking shift of $\Delta a/a = -0{\cdot}1642$, ideally $-1/6$.

The intensity data used in refining the atomic coordinates were collected about the [100]- and [110]-zone axes, employing a Weissenberg camera and Mo-$K\alpha$ radiation. Visual estimates were made of 420 reflections, about four times the number recorded in the previous investiga-

tion. No correction was made for absorption; its maximum effect on the intensity measurements was calculated to be less than 3 %.

The refinement was carried out by means of two-dimensional difference syntheses, beginning with the final coordinates of the earlier work. The structure-factor computations and Fourier syntheses were performed on EDSAC II using the scattering factors of Berghuis *et al.* (1955). Ten refinement cycles were calculated for both the (100) and (110) projections with small adjustments being applied to the atomic coordinates and temperature factors at the completion of each cycle. The initial coordinates gave an R factor of 20·2 %, which was reduced to 7·5 % for the coordinates given in table I. The interatomic distances and bond angles in table II were computed from the arithmetic mean of the (100) and (110) coordinates. The final structure factors listed in table III were calculated using the temperature factors $B_{\mathrm{Si}} = 0{\cdot}70$, $B_{\mathrm{Al}} = 0{\cdot}80$, and $B_{\mathrm{O}} = 1{\cdot}15$ Å^2. Electron-density maps calculated with the observed structure-factor amplitudes are shown in figs. 1*a* and 1*b*. Except for some juxtaposition in the basal oxygen layer (O_1, O_2, and O_3), the resolution of atoms in the two projections is excellent; one of the unsatisfactory features of the earlier analysis was the extensive overlap in the (010) projection.

The accuracy of the structure determination was assessed in three ways. The standard deviation of the coordinates was first estimated from the root-mean-square slope of the final difference maps, using the expression

$$\hat{\sigma}(x_n) = 2\{\overline{[\partial(\rho_o - \rho_c)/\partial x]}\}^{\frac{1}{2}}/C_n,$$

where ρ_o and ρ_c are the observed and calculated electron densities, and $C_n = \partial^2\rho_o/\partial x_n^2$, the central curvature of the nth atom evaluated from an F_o synthesis (method 1). Assuming $\sigma(F_o) = K|F_o|$, corroborating evidence for the experimental error was then obtained from

$$\hat{\sigma}(x_n) = \pi K\Big(\sum_{n=1}^{N} Z_n^2/2A\Big)^{\frac{1}{2}}/pZ_n,$$

in which Z_n is the atomic number, A the area of the projection, and p a function of the atomic shape (method 2). The constant K was taken as 0·1 following the suggestion of Lipson and Cochran (1953), who have described both methods in some detail. A third estimate of the error was obtained from the deviation of the three measurements of z (cf. table I) from their mean $\bar{z}$:

$$\hat{\sigma}(z_n) = c\Big[\sum_{i=1}^{3} (\bar{z}-z_i)^2\Big]^{\frac{1}{2}}/2 \text{ (method 3).}$$

TABLE I. Atomic coordinates in cell fractions.

	(100) projection		(110) projection*				Mean values		
Atom	y	z	x	y	z	z	x	y	z
Si_1	0·4006	0·0409	0·0117	0·3995	0·0406	0·0401	0·0117	0·4001	0·0405
Si_2	0·5733	0·0408	0·5002	0·5731	0·0402	0·0397	0·5002	0·5732	0·0402
Al_1	0·2520	0·2329	0·9154	0·2548	0·2314	0·2316	0·9154	0·2534	0·2320
Al_2	0·4175	0·2311	0·4190	0·4164	0·2301	0·2306	0·4190	0·4170	0·2306
O_1	0·2360	0·9940	0·9554	0·2385	0·9932	0·9946	0·9554	0·2373	0·9939
O_2	0·4708	0·9935	0·2587	0·4740	0·9956	0·9934	0·2587	0·4724	0·9942
O_3	0·5080	0·0068	0·7646	0·5130	0·0042	0·0064	0·7646	0·5105	0·0058
O_4	0·3889	0·1529	0·0803	0·3863	0·1512	0·1529	0·0803	0·3876	0·1523
O_5	0·5820	0·1522	0·5110	0·5805	0·1525	0·1530	0·5110	0·5813	0·1526
$(OH)_1$	0·2746	0·1579	0·5818	0·2769	0·1573	0·1569	0·5818	0·2758	0·1574
$(OH)_2$	0·2736	0·2962	0·2439	0·2729	0·2948	0·2935	0·2439	0·2733	0·2948
$(OH)_3$	0·3945	0·2988	0·7472	0·3953	0·2983	0·2973	0·7472	0·3949	0·2981
$(OH)_4$	0·5843	0·2965	0·3328	0·5820	0·2968	0·2955	0·3328	0·5832	0·2963

* Each atom appears twice in the (110) projection: at $(-x+y, z)$ and $(-x-y, z+\frac{1}{2})$.

TABLE II. Interatomic distances in Å. and bond angles in degrees.

Interatomic distances.

Silicon–oxygen, $\sigma = 0{\cdot}017$ Å.

Si_1–O_1	1·61	Si_2–O_1	1·63
Si_1–O_2	1·63	Si_2–O_2	1·62
Si_1O_3	1·63	Si_2–O_3	1·60
Si_1O_4	1·61	Si_2–O_5	1·62

Aluminium–oxygen, $\sigma = 0{\cdot}018$ Å.

Al_1–O_4	1·93	Al_2–O_4	1·98
Al_1–O_5	2·01	Al_2–O_5	1·94
Al_1–$(OH)_1$	1·93	Al_2–$(OH)_1$	1·90
Al_1–$(OH)_2$	1·83	Al_2–$(OH)_2$	1·88
Al_1–$(OH)_3$	1·86	Al_2–$(OH)_3$	1·86
Al_1–$(OH)_4$	1·86	Al_2–$(OH)_4$	1·85

Oxygen–oxygen, $\sigma = 0{\cdot}021$ Å.

Si_1 tetrahedron		Si_2 tetrahedron	
O_1–O_2	2·60	O_1–O_2	2·59
O_1–O_3	2·64	O_1–O_3	2·58
O_1–O_4	2·68	O_1–O_5	2·68
O_2–O_3	2·59	O_2–O_3	2·63
O_2–O_4	2·66	O_2–O_5	2·67
O_3–O_4	2·72	O_3–O_5	2·67
Al_1 octahedron		Al_2 octahedron	
O_4–O_5	2·76	O_4–O_5	2·81
O_4–$(OH)_1$	2·77	O_4–$(OH)_1$	2·76
O_4–$(OH)_2$	2·37*	O_4–$(OH)_2$	2·37*
O_4–$(OH)_3$	2·87	O_4–$(OH)_4$	2·90
O_5–$(OH)_1$	2·82	O_5–$(OH)_1$	2·76
O_5–$(OH)_2$	2·84	O_5–$(OH)_3$	2·84
O_5–$(OH)_4$	2·36*	O_5–$(OH)_4$	2·36*
$(OH)_1$–$(OH)_3$	2·36*	$(OH)_1$–$(OH)_2$	2·79
$(OH)_3$–$(OH)_4$	2·84	$(OH)_1$–$(OH)_3$	2·36*
$(OH)_2$–$(OH)_3$	2·79	$(OH)_2$–$(OH)_3$	2·80
$(OH)_3$–$(OH)_4$	2·72	$(OH)_2$–$(OH)_4$	2·81
$(OH)_3$–$(OH)_4$	2·82	$(OH)_3$–$(OH)_4$	2·72

* Shared edges.

Across vacant octahedral site

O_4–O_5	3·41	$(OH)_2$–$(OH)_2$	3·39
O_4–$(OH)_1$	3·47	$(OH)_2$–$(OH)_4$	3·47
O_5–$(OH)_1$	3·41	$(OH)_2$–$(OH)_4$	3·46

Interlayer distances

$(OH)_2$–O_1	2·94	$(OH)_4$–O_2	2·97
$(OH)_2$–O_3	3·12		

Interatomic angles.

Oxygen–silicon–oxygen, $\sigma = 0{\cdot}9°$

O_1–Si_1–O_2	106·9	O_1–Si_2–O_2	105·8
O_1–Si_1–O_3	109·2	O_1–Si_2–O_3	105·9
O_1–Si_1–O_4	111·8	O_1–Si_2–O_5	111·3
O_2–Si_1–O_3	104·9	O_2–Si_2–O_3	109·5
O_2–Si_1–O_4	110·1	O_2–Si_2–O_5	111·5
O_3–Si_1–O_4	113·8	O_3–Si_2–O_5	112·6

Silicon–oxygen–silicon, $\sigma = 1{\cdot}0°$

Si_1–O_1–Si_2	128·8	Si_1–O_3–Si_2	141·8
Si_1–O_2–Si_2	131·0		

Silicon–oxygen–aluminium, $\sigma = 0{\cdot}9°$

Si_1–O_4–Al_1	125·5	Si_2–O_5–Al_1	128·7
Si_1–O_4–Al_2	129·5	Si_2–O_5–Al_2	124·4

Oxygen–aluminium–oxygen, $\sigma = 0{\cdot}8°$

O_4–Al_1–O_5	89·0	O_4–Al_2–O_5	91·5
O_4–Al_1–$(OH)_1$	91·7	O_4–Al_2–$(OH)_1$	90·7
O_4–Al_1–$(OH)_2$	77·9	O_4–Al_2–$(OH)_2$	75·6
O_4–Al_1–$(OH)_3$	98·5	O_4–Al_2–$(OH)_2$	165·9
O_4–Al_1–$(OH)_4$	162·2	O_4–Al_2–$(OH)_4$	98·7
O_5–Al_1–$(OH)_1$	91·3	O_5–Al_2–$(OH)_1$	91·7
O_5–Al_1–$(OH)_2$	94·9	O_5–Al_2–$(OH)_2$	165·5
O_5–Al_1–$(OH)_3$	166·4	O_5–Al_2–$(OH)_3$	96·8
O_5–Al_1–$(OH)_4$	75·2	O_5–Al_2–$(OH)_4$	77·2
$(OH)_1$–Al_1–$(OH)_2$	168·0	$(OH)_1$–Al_2–$(OH)_2$	95·1
$(OH)_1$–Al_1–$(OH)_3$	77·1	$(OH)_1$–Al_2–$(OH)_3$	77·8
$(OH)_1$–Al_1–$(OH)_4$	97·0	$(OH)_1$–Al_2–$(OH)_4$	165·5
$(OH)_2$–Al_1–$(OH)_3$	97·9	$(OH)_2$–Al_2–$(OH)_3$	97·2
$(OH)_2$–Al_1–$(OH)_4$	94·8	$(OH)_3$–Al_2–$(OH)_4$	97·9
$(OH)_3$–Al_1–$(OH)_4$	98·7	$(OH)_3$–Al_2–$(OH)_4$	94·2

Aluminium–oxygen–aluminium, $\sigma = 0{\cdot}9°$

Al_1–O_4–Al_2	99·3	Al_1–$(OH)_2$–Al_2	106·9
Al_1–O_5–Al_2	99·1	Al_1–$(OH)_3$–Al_2	104·6
Al_1–$(OH)_1$–Al_2	100·5	Al_1–$(OH)_4$–Al_2	108·6

TABLE III. Comparison of observed and calculated structure factors. (100) projection

k.	*l.*	*Fo.*	|*Fc.*|	*k.*	*l.*	*Fo.*	|*Fc.*|	*k.*	*l.*	*Fo.*	|*Fc.*|	*k.*	*l.*	*Fo.*	|*Fc.*|
0	0	*	52	4	7	24	26	8	4	11	10	12	8	4	4
	4	79	85		8	36	37		5	12	12		9	7	7
	6	42	40		9	23	24		6	8	8		10	14	14
	8	43	44		10	20	21		7	9	8		11	7	7
	10	32	37		11	7	5		8	12	11		12	9	8
	12	36	41		12	23	25		9	9	8		13	8	7
	14	24	27		13	9	9		10	8	7		14	7	7
	16	37	43		14	14	14		11	14	14		15	7	7
	18	10	9		15	4	3		12	11	11		16	13	10
	20	24	24		16	12	12		13<	4	4		17	8	7
	22	9	10		17	8	7		14	10	10		18<	4	3
	24	7	8		18	14	13		15	13	13		19	8	8
	26	18	16		19	6	6		16	5	4		20	6	6
	28	11	9		20<	4	4		17<	4	4		21	5	6
	30	7	5		21	5	6		18	4	6		22<	4	5
	32	6	5	6	0	76	79	10	0	12	11		23	4	5
2	0	18	16		1	13	13		1	12	12	14	0<	4	1
	1	32	30		2	33	33		2	7	8		1	4	4
	2	44	44		3	15	15		3	11	11		2<	4	2
	3	17	16		4	30	32		4	11	11		3<	4	3
	4	26	24		5	11	11		5	8	7		4<	4	3
	5	13	13		6	21	23		6	8	7		5	7	6
	6	20	21		7	14	14		7	20	20		6<	4	1
	7	5	6		8	16	16		8	18	17		7	6	5
	8	17	18		9	13	13		9	17	17		8<	4	4
	9	9	9		10	33	35		10	5	4		9<	4	2
	10	7	8		11	11	11		11	5	5		10<	4	1
	11	13	14		12	30	32		12	9	9		11	5	5
	12	13	14		13	9	9		13	5	6	16	0	4	3
	13	12	11		14	16	18		14<	4	2		1	9	7
	14	10	10		15	6	6		15	4	6		2<	4	1
	15	10	11		16	31	33		16	4	4		3	5	6
	16<	4	2		17	7	6		17	6	7		4<	4	2
	17	7	8		18	4	4		18<	4	5		5<	4	3
	18	10	9		19	5	6		19	12	10		6	4	3
	19<	4	3		20	19	17		20	5	5		7	13	10
	20	4	5		21<	4	3		21	4	3		8	5	5
	21<	4	4		22	5	7		22<	4	1		9	12	8
	22	5	5		23<	4	3		23	6	6		10	4	2
	23<	4	2		24	5	5	12	0	24	23	18	0<	4	4
	24	5	5		25<	4	2		1	15	13		1	9	6
4	0	7	5		26	13	11		2	7	8		2<	4	2
	1	7	6		27<	4	3		3	15	14		3	10	7
	2	14	12		28	7	6		4	17	16		4	5	5
	3	14	15	8	0	8	10		5	9	9		5<	4	5
	4	32	32		1	18	18		6	14	14		6<	4	5
	5	21	21		2	5	6		7	10	9		7	5	5
	6	10	9		3	9	8								

* Not observed.

TABLE III (*cont.*)

(110) projection ($h = -k'$, $k = k'$)

k'.	l.	$Fo.$	$\lvert Fc.\rvert$	k'.	l.	$Fo.$	$\lvert Fc.\rvert$	k'.	l.	$Fo.$	$\lvert Fc.\rvert$	k'.	l.	$Fo.$	$\lvert Fc.\rvert$
0	2	*	52	1	$\bar{13}$	10	10	3	0	8	7	4	0	16	14
	4	82	85		$\bar{14}$	7	7		1	77	79		1	20	18
	6	45	40		$\bar{15}$	10	10		2	6	7		2	11	11
	8	48	44		$\bar{16}$	11	12		3	42	42		3	14	14
	10	35	36		$\bar{17}$	12	12		4	7	7		4<	4	2
	12	40	41		$\bar{18}$<	4	1		5	27	28		5	6	6
	14	26	27		$\bar{19}$	8	8		6	6	6		6	16	16
	16	42	42		$\bar{20}$	7	7		7	30	31		7	10	8
	18	10	10		$\bar{21}$	8	9		8	8	8		8	12	11
	20	22	23		$\bar{22}$<	4	1		9	20	19		9	5	4
	22	9	11		$\bar{23}$	4	4		10	9	9		10	17	18
	24	9	8	2	0	10	9		11	36	38		11	10	10
	26	14	16		1	8	7		12	9	8		12	17	18
	28	9	9		2	16	15		13	32	34		13	10	9
	30	4	5		3	5	5		14	8	8		14	11	11
1	0	32	32		4	25	23		15	16	15		15	8	6
	1	36	36		5	23	23		16	5	5		16	15	14
	2	23	22		6	20	20		17	32	32		17	8	8
	3	34	31		7	24	25		18	4	5		18	7	7
	4	21	19		8	39	39		19<	4	6		19<	4	2
	5	29	28		9	25	25		20	4	3		20	8	8
	6	4	3		10	17	16		21	14	13	4	$\bar{1}$	11	8
	7	11	11		11	10	11		22<	4	2		$\bar{2}$	8	7
	8	11	10		12	27	28		23	7	7		$\bar{3}$	7	6
	9	16	17		13	7	7		24<	4	1		$\bar{4}$	12	14
	10	6	7		14	15	15		25<	4	3		$\bar{5}$	7	7
	11	13	13		15<	4	4		26<	4	1		$\bar{6}$	14	15
	12	15	14		16	16	16		27	11	10		$\bar{7}$	4	3
	13<	4	4		17<	4	3		28<	4	1		$\bar{8}$	13	13
	14	11	11		18	10	9		29	10	8		$\bar{9}$	12	12
	15	12	13		19	9	8	3	$\bar{1}$	26	27		$\bar{10}$	17	19
	16	11	10		20<	4	4		$\bar{2}$	9	10		$\bar{11}$	7	7
	17	8	8		21	9	7		$\bar{3}$	35	38		$\bar{12}$	7	7
	18	4	5		22<	4	6		$\bar{4}$	6	6		$\bar{13}$	8	8
	19	10	10		23	7	6		$\bar{5}$	23	27		$\bar{14}$	10	12
	20	6	5	2	$\bar{1}$	6	5		$\bar{6}$	7	10		$\bar{15}$	5	7
	21	11	10		$\bar{2}$	13	14		$\bar{7}$	22	22		$\bar{16}$	8	8
	22<	4	4		$\bar{3}$	20	19		$\bar{8}$	6	6		$\bar{17}$<	4	2
	23<	4	4		$\bar{4}$	34	30		$\bar{9}$	37	41		$\bar{18}$	4	5
	24<	4	2		$\bar{5}$	22	24		$\bar{10}$<	4	5	5	0	4	3
	25	5	6		$\bar{6}$	23	23		$\bar{11}$	22	25		1	10	10
	26	4	5		$\bar{7}$	29	30		$\bar{12}$	4	2		2	10	9
	27	4	3		$\bar{8}$	26	27		$\bar{13}$	22	25		3	5	4
1	$\bar{1}$	48	47		$\bar{9}$	9	11		$\bar{14}$<	4	1		4	4	5
	$\bar{2}$	22	21		$\bar{10}$	24	24		$\bar{15}$	27	31		5<	4	3
	$\bar{3}$	22	20		$\bar{11}$	9	9		$\bar{16}$<	4	2		6	15	14
	$\bar{4}$	12	11		$\bar{12}$	18	19		$\bar{17}$<	4	2		7	12	11
	$\bar{5}$	25	24		$\bar{13}$<	4	3		$\bar{18}$<	4	5		8	16	15
	$\bar{6}$	11	9		$\bar{14}$	13	13		$\bar{19}$	12	16		9	15	14
	$\bar{7}$	12	12		$\bar{15}$	4	4		$\bar{20}$	4	3		10	19	19
	$\bar{8}$	9	7		$\bar{16}$	8	9		$\bar{21}$<	4	7		11<	4	1
	$\bar{9}$	10	10		$\bar{17}$	7	7		$\bar{22}$<	4	4		12<	4	5
	$\bar{10}$	12	12		$\bar{18}$	9	9		$\bar{23}$<	4	6		13	6	6
	$\bar{11}$	17	19		$\bar{19}$	9	8		$\bar{24}$<	4	3		14<	4	4
	$\bar{12}$	14	14		$\bar{20}$	7	7		$\bar{25}$	10	12		15<	4	2

* Not observed.

TABLE III (*cont.*)
(110) projection ($h = -k'$, $k = k'$)

k'.	l.	*Fo.*	$\|Fc.\|$	k'.	l.	*Fo.*	$\|Fc.\|$	k'.	l.	*Fo.*	$\|Fc.\|$	k'.	l.	*Fo.*	$\|Fc.\|$
5	16<	4	3	6	2	27	27	6	$\bar{7}$	4	4	7	$\bar{7}$	4	6
	17	8	7		3	9	7		$\bar{8}$	15	17	8	0<	4	2
	18<	4	0		4	16	15		$\bar{9}$	4	4		1<	4	2
	19<	4	5		5	9	8		$\bar{10}$	5	6		2<	4	3
	20<	4	4		6	15	14		$\bar{11}$<	4	4		3<	4	4
	21<	4	2		7	5	6		$\bar{12}$	10	10		4<	4	3
	22	10	9		8	19	20		$\bar{13}$<	4	4		5	4	2
5	$\bar{1}$	7	6		9	4	5		$\bar{14}$	12	12		6<	4	2
	$\bar{2}$	10	9		10<	4	1		$\bar{15}$	4	5		7	6	5
	$\bar{3}$	13	13		11<	4	5		$\bar{16}$<	4	1		8	4	2
	$\bar{4}$	16	16		12	15	14		$\bar{17}$<	4	6		9	7	5
	$\bar{5}$	5	5		13<	4	4		$\bar{18}$	8	10		10	9	6
	$\bar{6}$	22	22		14	10	11		$\bar{19}$<	4	3		11	10	8
	$\bar{7}$	12	13		15<	4	5		$\bar{20}$	4	5	8	$\bar{1}$<	4	3
	$\bar{8}$	5	6		16<	4	3	7	0<	4	1		$\bar{2}$<	4	4
	$\bar{9}$	6	6		17<	4	4		1	5	6		$\bar{3}$	6	7
	$\bar{10}$	7	8		18	11	11		2	4	5		$\bar{4}$<	4	3
	$\bar{11}$	7	8		19<	4	3		3	4	4		$\bar{5}$	10	9
	$\bar{12}$<	4	3		20<	4	7		4	5	5	9	0	4	4
	$\bar{13}$<	4	2		21<	4	3		5<	4	3		1<	4	2
	$\bar{14}$	7	7		22<	4	5		6<	4	3		2	4	4
	$\bar{15}$	5	4		23<	4	3		7	7	6		3	7	7
	$\bar{16}$	7	7		24	9	8		8	7	6		4	6	3
	$\bar{17}$	5	6	6	$\bar{1}$	7	8	7	$\bar{1}$<	4	3		5	4	4
	$\bar{18}$	6	6		$\bar{2}$	22	22		$\bar{2}$	4	4		6	4	4
	$\bar{19}$	6	6		$\bar{3}$	4	5		$\bar{3}$	7	7		7<	4	4
	$\bar{20}$	7	8		$\bar{4}$	12	14		$\bar{4}$	4	5		8	4	3
6	0<	4	4		$\bar{5}$	7	6		$\bar{5}$<	4	7		9	9	8
	1	7	8		$\bar{6}$	10	9		$\bar{6}$<	4	0	9	$\bar{1}$	11	9

The standard deviations of the coordinates are: method 1, Si 0·004 Å., Al 0·006 Å., O 0·013 Å.; method 2, Si 0·007 Å., Al 0·009 Å., O 0·015 Å.; method 3, Si 0·006 Å., Al 0·008 Å., O 0·010 Å., these results being averaged over the three crystallographic directions and over all atoms of the same element. The largest estimates of $\hat{\sigma}$, i.e. those of method 2, were applied in computing the standard deviations of the interatomic distances and bond angles given in table II. Differences in lengths or angles exceeding 2·3 σ were taken as significant in the discussion that follows.

Nature of the kaolin layer.

A single kaolin layer of the dickite structure is shown in fig. 2. There are two such layers in the unit cell, the second being related to the first by a *c*-glide symmetry plane. Within each kaolin layer, the silicon tetrahedral layer and the aluminium octahedral layer show considerable distortion from their idealized geometry, indicative of the strong interatomic forces exerted between them. Some of the deformation may be caused by the slight difference in natural size of the silica and alumina

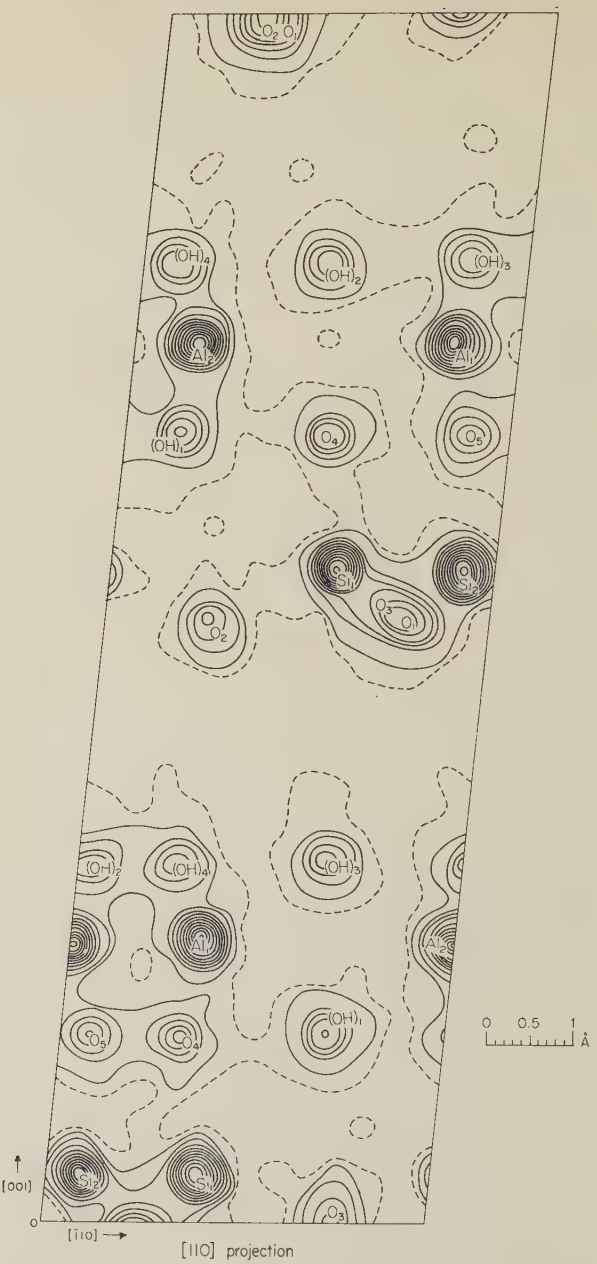

FIG. 1*a*. The [110] projection of the electron density in dickite, calculated with the observed structure amplitudes, $|Fo|$. Contours are drawn approximately at intervals of 2 electrons per Å^2.; the dashed contour is 1 electron per Å^2.

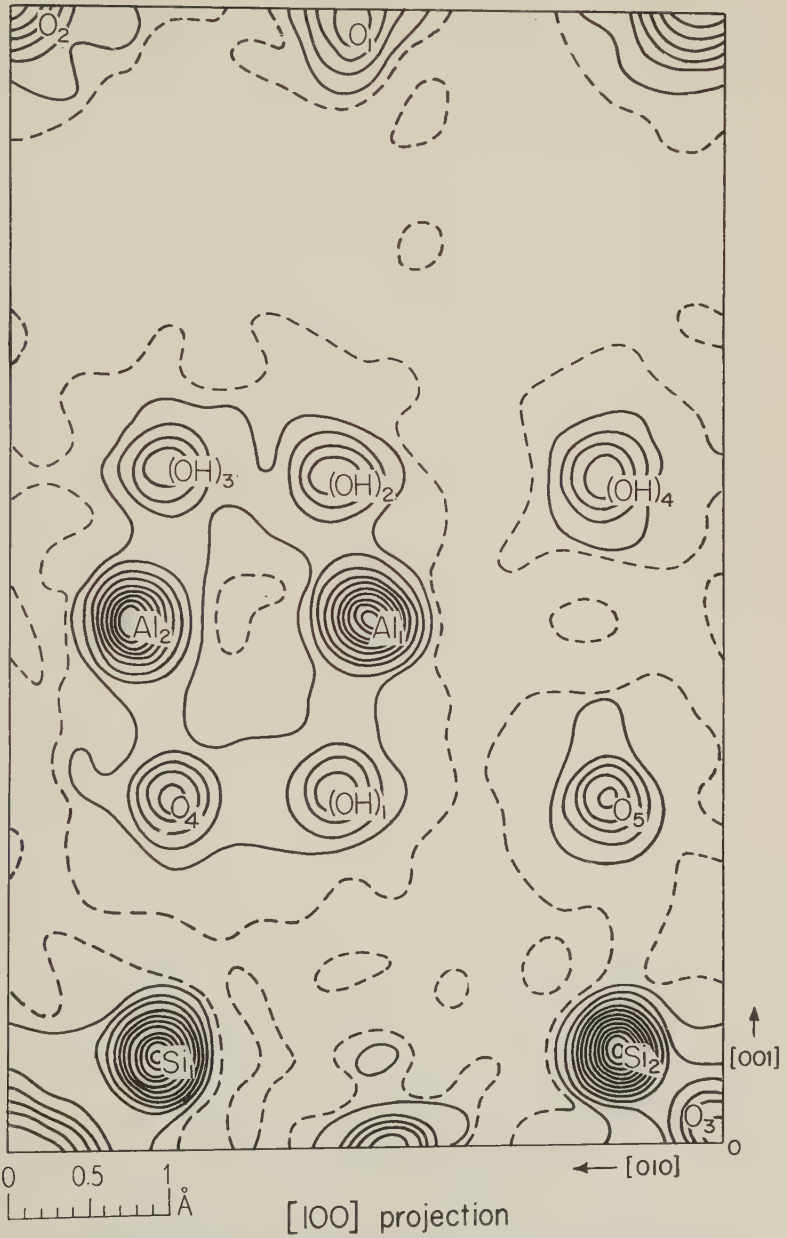

FIG. 1*b*. The [100] projection of the electron density in dickite. Details as in fig. 1*a*.

layers; the Al octahedral layer, as found in gibbsite for example, is somewhat smaller than a Si_2O_5 sheet with Si–O distances of 1·6 Å. Such a misfit would lead to tension in the octahedral layer and compression of the silica sheet. The resulting influence on the morphology of various layer-lattice silicates has been discussed by Bates (1959).

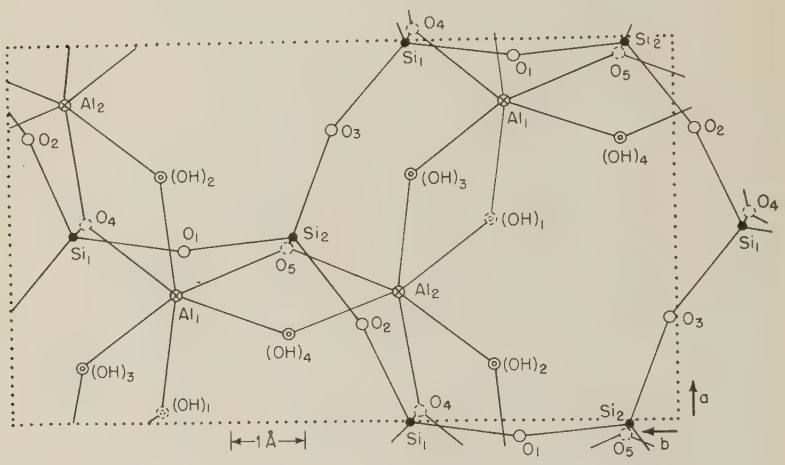

Fig. 2. A portion of the dickite kaolin-layer.

The silica layer is compressed through rotation of the tetraheda in (001). The Si_1 and Si_2 tetrahedra are rotated in opposite directions by about 7·5° with the directions of rotation apparently determined by the attractive force between Al_1 and O_1 and between Al_2 and O_2. Further evidence of compression in the silica layer is given by the observed deformation of individual tetrahedra. The O–O distances and O–Si–O bond angles show that the tetrahedra are contracted in the oxygen basal plane and elongated along c^*, normal to the basal plane. All distances and angles that involve the apex oxygens O_4 and O_5 are larger than those that do not. Despite this deformation, none of the silicon-oxygen bond lengths differ significantly from their arithmetic mean of 1·62 Å., slightly larger than the value $1{\cdot}60 \pm 0{\cdot}01$ recommended by Smith (1954). Recent refinements of coesite (Zoltai and Buerger, 1959) and danburite (Johannson, 1959) also show mean Si–O distances of 1·62 Å. Another feature of the silica sheet is the puckering in the basal oxygen plane. Atom O_3 is approximately 0·17 Å. higher than O_1 and O_2, thus causing corrugations running along [110] and $[1\bar{1}0]$ in alternate kaolin layers. These corrugations arise as a result of the

shortened shared edges in the Al octahedral layer. Oxygens O_4 and O_5 are shifted toward $(OH)_2$ and $(OH)_4$, respectively, causing the silica tetrahedra to be tilted in such a way as to depress O_1 and O_2 while elevating O_3.

The distortions in the Al layer are best illustrated by the three classes of oxygen -oxygen distances: the six O–O distances across the vacant octahedral site ranging between 3·39 and 3·47 Å. (mean 3·43 Å.), the eighteen unshared octahedral edges from 2·72 to 2·90 Å. (mean 2·80 Å.), and the three shared octahedral edges of 2·37 Å. All twenty-seven distances would be equal if the octahedra were undistorted. The short shared edges are particularly striking since they are 0·1 Å. less than those observed in comparable structures. The shortest O–O distances found in gibbsite (Megaw, 1934) and diaspore (Busing and Levy, 1958) are 2·47 and 2·46 Å., respectively. The shortened shared edges arise as a consequence of the expansion of the Al–O,OH network and also exert a marked influence on the O–Al–O bond angles; those that subtend shared edges are about 20° smaller than the others. The aluminium ions are not equidistant from their nearest neighbours; the $Al–(OH)_{2,3,4}$ distances average 1·86 Å., while those to the O,OH layer have a mean of 1·95 Å. The irregular configurations and interatomic distances are very similar to those found in diaspore by Busing and Levy (1958). The Al atoms in dickite are closer to the hydroxyl layer than to the O,OH layer because of the repulsive forces originating from the Si ions. The effect is enhanced by the stretching forces acting on the octahedra, allowing greater freedom of motion for the aluminium cations. Al_2 is slightly lower than Al_1 since it lies directly beneath a silicon ion in the layer above.

Hydrogen positions and interlayer bonding.

The contacts between kaolin layers illustrated in fig. 3 show the hydroxyls and oxygens linked together in pairs. The $(OH)_2–O_1$ and $(OH)_4–O_2$ distances are 2·94 and 2·97 Å., respectively, while $(OH)_3–O_3$ is a significantly longer bond of 3·12 Å. because of the puckering of the oxygen layer. All other interlayer oxygen oxygen distances are greater than 3·5 Å. The rotation directions of the silica tetrahedra act to reduce the length of the OH O contacts. If the hydroxyls of one layer are rotated clockwise because of the shortened shared edges, then the oxygens of the adjacent kaolin layer also undergo a clockwise movement. This mechanism appears to be important in regard to polymorphism in kaolin minerals and will be discussed further in the next section.

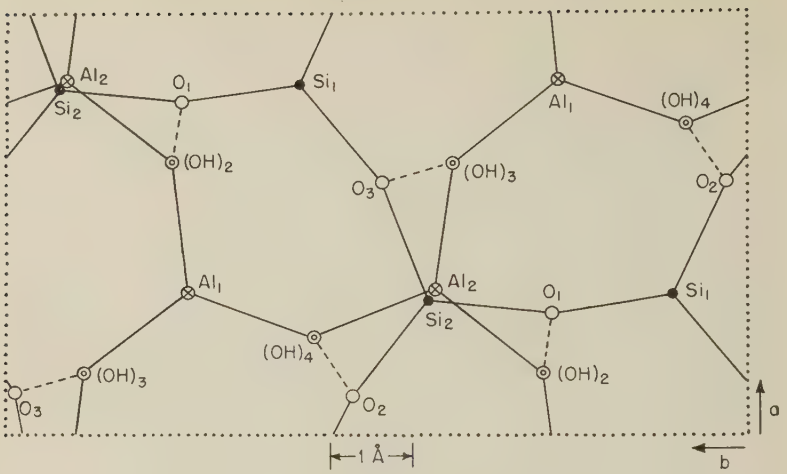

Fig. 3. Dickite interlayer bonding.

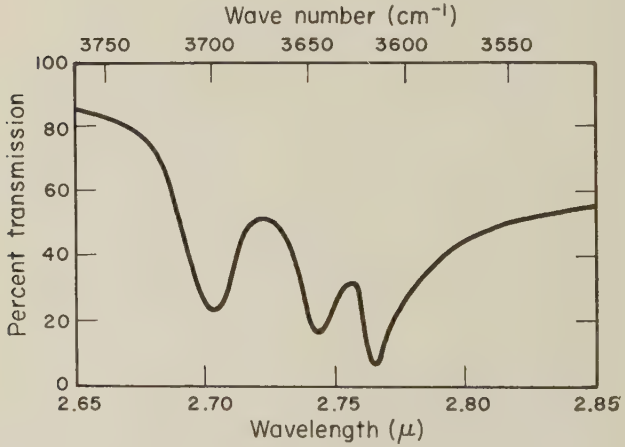

Fig. 4. Infra-red spectrograms of Schuylkill dickite.

The structure analysis was not sufficiently accurate to fix the hydrogen positions. In a survey of hydrogen-bearing compounds, McDonald (1956) has shown that the peak heights of hydrogen atoms range from 0·7 to 1·0 electrons per Å^2. An F_o or (F_o-F_c) synthesis for non-centrosymmetric dickite might therefore be expected to show maxima of 0·5 electrons per Å^2. at the hydrogen positions. Unfortunately such detail was obscured by spurious background; the final F_o projections (figs. 1*a* and 1*b*) gave a standard deviation in the electron density of 0·3 elec-

trons per Å^2. There are, however, small maxima in the interlayer region which are suggestive of hydrogen atoms. A three-dimensional analysis, with counter data for the low-angle reflections, is probably necessary to resolve the question.

Less ambiguous information regarding the disposition of the hydrogen atoms was obtained from the OH–O infra-red vibration spectra of Schuylkill dickite. The mineral was prepared as a mull in high-boiling paraffin (Nujol) and 'Perfluorolube' and mounted between glass cover

TABLE IV. Infra-red absorption data for Schuylkill dickite.

Wavelength (μ)	Wave number (cm.$^{-1}$)	Relative intensity	Proposed structure	O–O distance (Å.)
$2{\cdot}70_3$	370_0	medium	$(O–H)_1$	—
$2{\cdot}74_4$	364_4	medium	$(O–H)_3—O_3$	3·12
$2{\cdot}76_5$	361_7	strong	$(O–H)_2—O_1$	2·97
			$(O–H)_4—O_2$	2·94

slides. Microscopic examination showed that most of the dickite crystals were oriented parallel to (001), despite extensive grinding. Excellent resolution of the important absorption bands near 3 700 cm.$^{-1}$ (fig. 4) was obtained with a Beckman DK-1 instrument, employing a quartz optical system. The wave-lengths of the dickite absorption spectra listed in table IV were calibrated with the polyethylene absorption band at 3·508 μ. It is unlikely that any of the dickite bands are due to adsorbed water since identical results were obtained with specimens heated at 400° C. In a previous investigation (Adler *et al.*, 1950) of dickite from St. George, Utah, U.S.A., and San Juanita, Mexico, infra-red absorption spectra were found at 2·73, 2·83, and 3·33 μ.

Tentative structural assignments for the OH–O stretching frequencies are proposed in table IV. The choices are somewhat arbitrary but are based on the survey of Nakamoto *et al.* (1955), in which the infra-red vibration frequencies of a large number of hydrogen-bonded compounds have been correlated with pertinent interatomic distances. The proposed model places the hydrogen atoms of $(OH)_2$, $(OH)_3$, and $(OH)_4$ on long hydrogen bonds that connect the hydroxyl groups to their closest oxygen neighbours in the adjacent kaolin layer, while $(OH)_1$ functions primarily as a free hydroxyl group.

Polymorphism in kaolin minerals.

Three polymorphic forms of kaolin-layer silicates are found in nature: kaolinite, dickite, and nacrite. In addition to these crystalline varieties, there are a number of minerals showing a more or less irregular sequence

of kaolin layers. As pointed out by Hendricks (1938), the key feature of the interlayer coordination is the manner in which oxygens and hydroxyls approach one another in pairs to form long hydrogen bonds. The type of stacking translations that leads to the required interlayer bonding (table V) was determined by Brindley (1951). His analysis gives an adequate account of the possible one-layer structures, but it cannot be applied to multi-layer unit cells in which consecutive kaolin layers are rotated with respect to one another.

TABLE V. Translations of the base-centred unit cell leading to paired oxygen-hydroxyl bonds (after Brindley, 1951). The numbers refer to the stacking sequences of table VI and fig. 8.

		$\Delta b/b$.						
		$-\frac{1}{2}$.	$-\frac{1}{3}$.	$-\frac{1}{6}$.	0.	$+\frac{1}{6}$.	$+\frac{1}{3}$.	$+\frac{1}{2}$.
$\Delta a/a$	$-\frac{1}{2}$	1	—	31	—	19	—	1
	$-\frac{1}{3}$	—	13	—	7	—	25	—
	$-\frac{1}{6}$	—	—	—	—	—	—	—
	-0	—	19	—	1	—	31	—
	$+\frac{1}{6}$	7	—	25	—	13	—	7
	$+\frac{1}{3}$	—	—	—	—	—	—	—
	$+\frac{1}{2}$	1	—	31	—	19	—	1

In order to determine all the permissible stacking sequences for two kaolin layers, the primitive unit cell shown in fig. 5 was chosen as a reference. The six different ways in which the oxygens of the next kaolin layer can be paired with the hydroxyls of the reference cell are illustrated in fig. 6. For each of the six possibilities there are six ways to construct the second kaolin layer; these are related to one another by a rotation angle ϕ (fig. 7). Thus there are $6 \times 6 = 36$ different superposition patterns for two kaolin layers. The situation is somewhat more complex than that of the mica family (Smith and Yoder, 1956), where there are only six different stacking sequences. Fig. 8 shows the thirty-six permissible second layers for the reference cell of fig. 5; their stacking shifts and rotation angles are given in table VI. Six of these sequences (for which $\phi = 0$) are identical with those proposed by Brindley (cf. table V). Interlayer shifts related by unit-cell translations or the C-face centring operation are of course identical.

In constructing a unit cell of n kaolin layers from the permitted stacking sequences, the reference axes in the nth layer must maintain the same orientation as those in the origin layer. In other words, $\phi_1 - \phi_2 + \ldots + \phi_n = 2\pi N$, where N is an integer. For a one-layer cell, only those sequences that have $\phi = 0$ need be considered; in two-layer cells such as dickite, $\phi_1 + \phi_2 = 0$ or 2π. With the thirty-six stacking sequences of

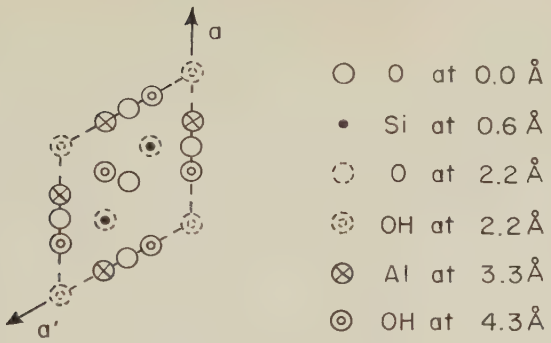

FIG. 5. Primitive reference cell.

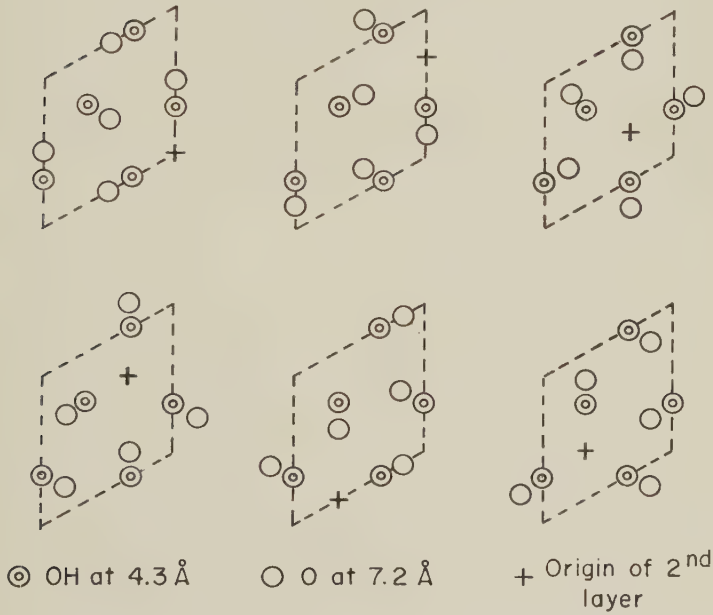

FIG. 6. Six ways of placing the oxygen layer over the hydroxyl layer.

table VI, six one-layer and 108 two-layer unit cells can be constructed. The discussion that follows attempts to justify nature's preference for only a small group of these polymorphic varieties. This objective can be accomplished with the following assumptions concerning the most stable configurations: the highly charged Si^{4+} and Al^{3+} cations tend to avoid one another as much as possible; oxygens and hydroxyls approach one another as close as possible to promote strong interlayer bonding.

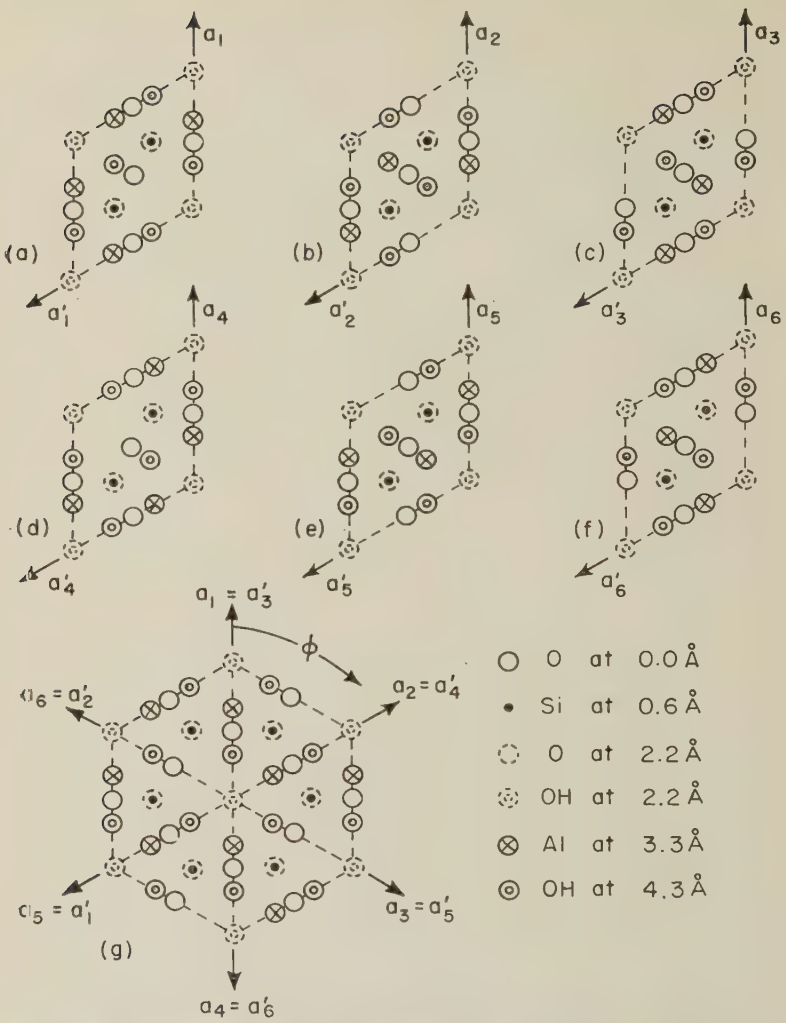

FIG. 7. The six methods, (*a*) -(*f*), of constructing a kaolin layer from a given basal oxygen network; (*g*) shows how the cells can be related by a rotation angle ϕ.

The first of these assumptions reduces the contribution of the cations to the Coulomb energy of the crystal; it can be applied to the stacking sequences of table VI by eliminating those with the greatest amount of cation–cation superposition in consecutive layers. The superimposed cations are enumerated in table VI, from which it can be seen that at least one-fourth of the second-layer cations are vertically coincident

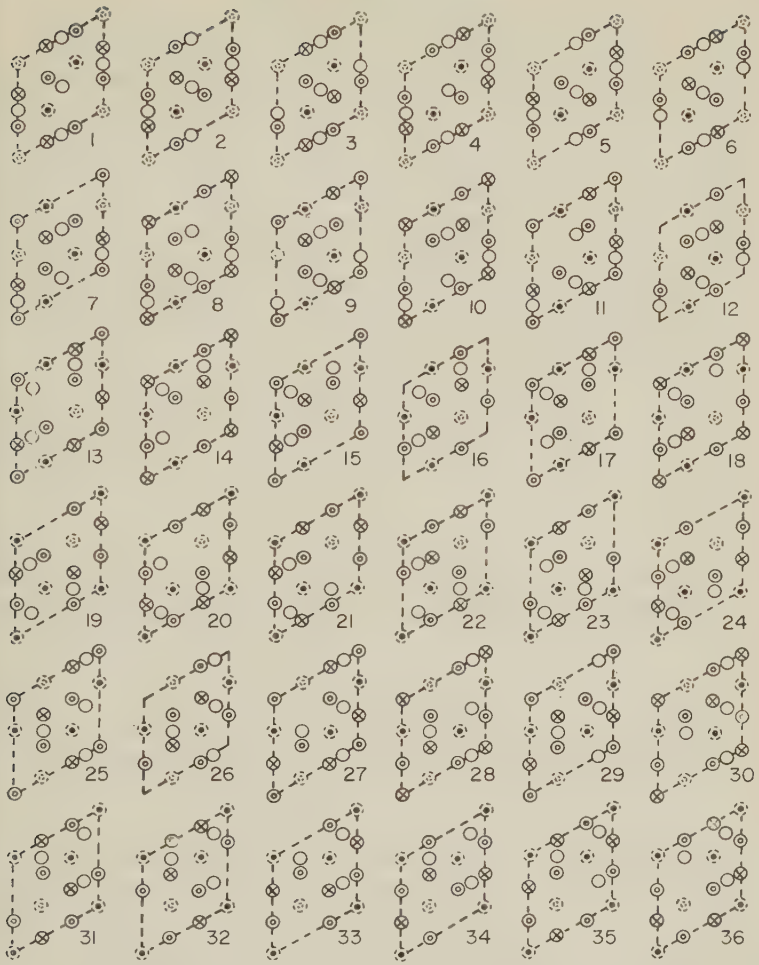

FIG. 8. Thirty-six possible second layers for the reference cell in fig. 5.

with those of the reference cell. If the stacking arrangements showing more than the minimum amount of overlap are rejected as energetically unfavourable, the following twelve remain: 7, 9, 11, 20, 22, 24, 25, 27, 29, 32, 34, and 36. The two one-layer and twelve two-layer cells that can be constructed from these stacking sequences are given in table VII.

The two single-layer cells are those of kaolinite and its mirror image, perhaps more properly designated as right- and left-handed kaolinite. The

TABLE VI. The thirty-six stacking sequences and their relationship with the reference cell.

No.	Interlayer shift and rotation angle Δa a	$\Delta a'$ a'	ϕ	Cation superposition Si_{II}–Si_I	Si_{II}–Al_I	Al_{II}–Si_I	Al_{II}–Al_I	Oxygen–hydroxyl approach Rotation	Pucker
1	0	0	0	1	0	0	1	U	F
2			1	1	0	0	0	F	U
3			2	1	0	0	½	U	U
4			3	1	0	0	0	F	F
5			4	1	0	0	½	U	U
6			5	1	0	0	0	F	U
7	⅔	0	0	0	½	0	0	F	U
8			1	0	½	½	0	U	F
9			2	0	½	0	0	F	U
10			3	0	½	½	0	U	U
11			4	0	½	0	0	F	F
12			5	0	½	1	0	U	U
13	⅓	⅓	0	0	1	0	0	F	F
14			1	0	1	½	0	U	U
15			2	0	1	0	0	F	U
16			3	0	1	1	0	U	F
17			4	0	1	0	0	F	U
18			5	0	1	½	0	U	U
19	⅔	⅓	0	½	0	0	½	U	U
20			1	½	0	0	0	F	F
21			2	½	0	0	1	U	U
22			3	½	0	0	0	F	U
23			4	½	0	0	½	U	F
24			5	½	0	0	0	F	U
25	0	⅔	0	0	½	0	0	F	U
26			1	0	½	1	0	U	U
27			2	0	½	0	0	F	F
28			3	0	½	½	0	U	U
29			4	0	½	0	0	F	U
30			5	0	½	½	0	U	F
31	⅓	⅔	0	½	0	0	½	U	U
32			1	½	0	0	0	F	U
33			2	½	0	0	½	U	F
34			3	½	0	0	0	F	U
35			4	½	0	0	1	U	U
36			5	½	0	0	0	F	F

Key: The interlayer translations are referred to the primitive unit cell of fig. 5, and the angle ϕ is expressed in multiples of $\pi/3$ radians. In the cation superposition columns, the digit '1' denotes complete coincidence of the cations in the second layer (II) over those of the reference cell (I). '½' and '0' mean that half or none of the cations are superimposed. Distortions that lead to close OH–O distances for a certain stacking sequence are denoted with an 'F' in the final two columns; 'U' signifies an unfavourable distortion.

relationship between these two structures, which contain stacking sequences 7 and 25 respectively, is shown in fig. 9. Kaolinite belongs to

TABLE VII. One- and two-layer unit cells formed from the stacking sequences with minimum cation superposition.

One-layer structures.	
7, 7, 7, 7, 7, . . .	25, 25, 25, 25, 25, . . .
Two-layer structures.	
7, 25, 7, 25, 7, . . .	22, 22, 22, 22, 22, . . .
34, 34, 34, 34, 34, . . .	22, 34, 22, 34, 22, . . .
9, 11, 9, 11, 9, . . .	9, 29, 9, 29, 9, . . .
11, 27, 11, 27, 11, . . .	27, 29, 27, 29, 27, . . .
20, 24, 20, 24, 20, . . .	20, 36, 20, 36, 20, . . .
24, 32, 24, 32, 24, . . .	32, 36, 32, 36, 32, . . .

the acentric triclinic point group 1, and may therefore show enantiomorphism (cf., for example, Henry *et al.* (1951)). In their analysis of the structure, Brindley and Robinson (1946*a*) chose the right-handed struc-

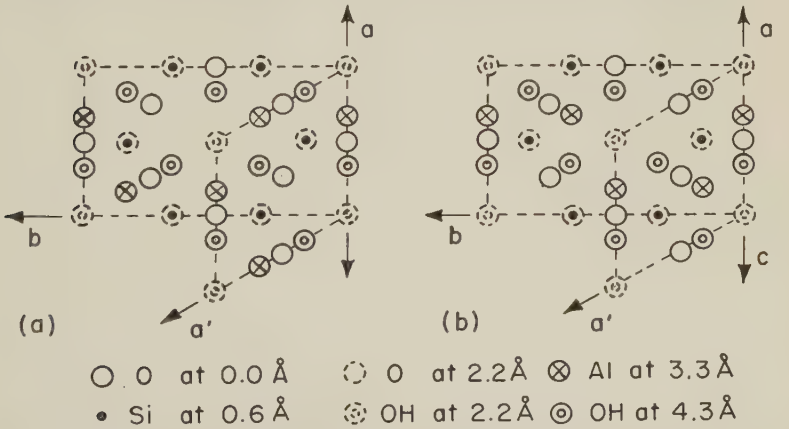

FIG. 9. The structure of (*a*) kaolinite, and (*b*) its mirror image, projected on (001). The α and γ angles of the mirror structure are supplementary to those of kaolinite.

ture (fig. 9*a*) as the correct solution, but its mirror image can be expected to give an identical X-ray diffraction pattern. An anomalous scattering experiment such as that performed on α-quartz by DeVries (1958), and additional physical information (e.g. morphology, etch patterns, or optical activity) would be required to distinguish the enantiomorphic pair. The experiment would be an extremely difficult one since kaolinite crystals are seldom larger than a few microns. Until the absolute configuration is determined it can only be assumed that every specimen of

kaolinite is a mixture of right- and left-handed crystals in unknown proportions. A random interleaving of the two modifications is also possible, in which case the diffraction pattern would show layers randomly displaced by multiples of $b/3$ (cf. table V). Such effects have been observed in English fireclays by Brindley and Robinson (1946*b*).

On the basis of the foregoing arguments concerning Coulomb energy, there is little to differentiate among the twelve two-layer cells of table VII. Secondary variations in the structures occur, however, when the effect of the kaolin-layer distortions on the interlayer bonding is considered. This criterion was first suggested by Brindley and Nakahira (1958) in their study of the triclinic distortions in kaolinite. The irregularities observed in dickite are likely to occur in any kaolin-layer sequence since interatomic forces within a layer are much stronger than those between layers. The most important features affecting the interlayer oxygen–hydroxyl distances are the rotation directions of the silica tetrahedra and the relationship between the pucker of the oxygen network and that of the adjoining hydroxyl sheet. Assuming the rotation directions to be determined by the disposition of aluminium ions, eighteen of the stacking sequences in table VI show longer OH–O contacts while those of the remaining eighteen are strengthened. Unfortunately, however, all twelve of the sequences with minimum cation cation superposition possess favourable angular rotations. When the puckering of the oxygen and hydroxyl layers is considered, four of the twelve sequences are clearly favoured. As mentioned previously, the buckling of the oxygen layer is caused by the shortened shared edges in the octahedral layer; as a result, the silica tetrahedra are tilted and atom O_3 becomes appreciably higher than O_1 and O_2. The hydroxyl layer also deviates from planarity because $(OH)_3$ shares a short octahedral edge with another hydroxyl group, whereas $(OH)_2$ and $(OH)_4$ are associated with the apex oxygens of the tetrahedral layer. $(OH)_3$ is therefore slightly elevated and the best interlayer linkage is obtained by matching O_3 with $(OH)_3$. The four sequences incorporating these $(OH)_1$–$(OH)_3$–O_3 groups are 11, 20, 27, and 36. Only two of the one- and two-layer unit cells in table VII are composed of the preferred arrangements: 11, 27, 11, 27, 11, . . ., and 20, 36, 20, 36, 20, ... The two-layer structures generated by these sequences are those of dickite and nacrite, respectively. Neither of the kaolinite structures satisfies the pucker criterion; this may explain why kaolinite crystals are seldom as large as those of dickite or nacrite. The crystal structure of nacrite was determined by Hendricks (1938); it is usually characterized as a six-layer pseudo-rhombohedral mineral but

only involves two types of stacking sequences alternating along the *c*-axis. Neither dickite nor nacrite shows enantiomorphism since both belong to the monoclinic point group *m*.

In summary, it has been shown that there are thirty-six stacking sequences which lead to the required interlayer bonding. Twelve of these arrangements are to be preferred if the cation superposition of consecutive layers is minimized. The twelve sequences generate two one-layer unit cells (kaolinite and its mirror image) and twelve two-layer cells (including dickite and nacrite). Unit cells containing more than two kaolin layers were not considered. When the effect of the kaolin layer distortions on the interlayer bonds is considered, the most stable configurations seem to be those of dickite and nacrite.

Acknowledgements. I wish to thank Dr. W. H. Taylor and Prof. A. R. von Hippel for provision of facilities and for their interest and encouragement. Thanks are also due to Messrs. M. Wells and B. Warner for programming the numerical calculations on EDSAC II of the Cambridge Mathematical Laboratory. The infra-red spectrograms were obtained with the assistance of Dr. A. Linz, Jr., and Mr. J. Kalnajs. The dickite specimen was supplied by Prof. G. W. Brindley, who also made several useful comments on the manuscript.

References.

Adler (H.), Bray (E. E.), Stevens (N. P.), Hunt (J. M.), Keller (W. D.), Pickett (E. E.), and Kerr (P. F.), 1950. Report 8, American Petroleum Institute Project 49, Columbia University, New York.

Bates (T. F.), 1959. Amer. Min., vol. 44, p. 78.

Berghuis (J.), Haanappel (IJ.), Potters (M.), Loopstra (B. O.), MacGillavry (C. H.), and Veenendaal (A. L.), 1955. Acta Cryst., vol. 8, p. 478.

Brindley (G. W.), 1951. X-ray identification and structure of the clay minerals, Min. Soc. Monograph, London, chap. 2.

—— and Nakahira (M.), 1958. Min. Mag., vol. 31, p. 781.

—— and Robinson (K.), 1946*a*. Ibid., vol. 27, p. 242.

—— —— 1946*b*. Trans. Faraday Soc., vol. 42B, p. 198.

Busing (W. R.) and Levy (H. A.), 1958. Acta Cryst., vol. 11, p. 798.

DeVries (A.), 1958. Nature, vol. 181, p. 1193.

Farquhar (M. C. M.) and Lipson (H.), 1946. Proc. Phys. Soc., vol. 58, p. 200.

Hendricks (S. B.), 1938. Zeits. Krist., vol. 100, p. 509.

Henry (N. F. M.), Lipson (H.), and Wooster (W. A.), 1951. The Interpretation of X-ray Diffraction Photographs. London (Macmillan and Co.), p. 161.

Honess (A. P.) and Williams (F. J.), 1935. Amer. Min., vol. 20, p. 462.

Johannson (G.), 1959. Acta Cryst., vol. 12, p. 522.

Lipson (H.) and Cochran (W.), 1953. The Determination of Crystal Structures, London (Bell & Sons Ltd.), chap. 9.

McDonald (T. R. R.), 1956. Acta Cryst., vol. 9, p. 162.

Megaw (H. D.), 1934. Zeits. Krist., vol. 87, p. 185.

Nakamoto (K.), Margoshes (M.), and Rundle (R. E.), 1955. Journ. Amer. Chem. Soc., vol. 77, p. 6480.

Newnham (R. E.) and Brindley (G. W.), 1956. Acta Cryst., vol. 9, p. 759; correction: ibid. 1957, vol. 10, p. 88.

Smith (J. V.), 1954. Acta Cryst., vol. 7, p. 479.

—— and Yoder (H. S.), 1956. Min. Mag., vol. 31, p. 209.

Weisz (O.), Cochran (W.), and Cole (W. F.), 1949. Acta Cryst., vol. 2, p. 280.

Zoltai (T.) and Buerger (M. J.), 1959. Zeits. Krist., vol. 111, p. 129.

A galena–wulfenite–uraniferous-asphaltite horizon in the Magnesian Limestone of Nottinghamshire.

By T. Deans, M.A., F.G.S.

Mineral Resources Division, Overseas Geological Surveys, London, W.C. 1.

[Read 31 March 1960.]

Summary. The top 2 inches of the Lower Magnesian Limestone is feebly but persistently mineralized along its outcrop from Nottingham to Doncaster, predominantly with galena and a little cerussite, frequently with uraniferous asphaltite containing 0·2 to 1 % U_3O_8. Wulfenite, both platy and pyramidal in habit, occurs at Bulwell and Kirkby in Ashfield. The mode of formation and the age of these minerals are discussed.

THE Permian rocks of northern England have long been known to contain small amounts of metallic sulphides, principally galena, blende, and pyrite, and while studying these, some ten years ago, a rather persistent galena horizon was recognized in the topmost inch or two of the Lower Magnesian Limestone, immediately below the impervious cover of the Middle Marl. Galena was seen at most of the accessible exposures of this horizon between its commencement at the Zechstein shoreline in Nottingham and the Don Valley near Doncaster, a distance of 40 miles. In 1958, while re-examining specimens of these rocks, two rather unexpected discoveries were made; firstly a black asphaltic mineral that often accompanied the galena was found to be radioactive, and secondly small crystals of wulfenite were recognized in several specimens. A few days' fieldwork in 1959 showed that both these minerals were fairly persistent in the Nottingham area, and the present paper is intended to bring these facts to the attention of those interested in the origin of English metalliferous deposits and in the peculiar geochemistry of Permian rocks. It should be added that the mineralization so far encountered is extremely low grade, nowhere approaching anything of economic interest, and the wulfenite crystals are very small.

Distribution and field relationships.

From the Geological Survey maps (10-mile, 1-inch, and 6-inch scales) the junction between the Lower Magnesian Limestone and the Middle

Permian Marl can be traced with precision from Nottingham northwards for 80 miles to Ripon, but exposures are rather few and often only temporary. Those yielding the minerals discussed here will be described in order from south to north, and defined by National Grid references.

Bulwell, Nottingham. At Bulwell Pottery (43/533452) the Middle Marl is worked for the manufacture of flower-pots, and formerly it was the practice to weather the clay by spreading it on the flat-lying surface of the Magnesian Limestone from which the Marl had previously been cleared. In 1950 three of these old weathering floors provided excellent exposures of the mineralized top layer of the Magnesian Limestone, everywhere showing a small percentage of finely disseminated galena. Adjacent to the Pottery, to the north-east, two limestone quarries also exposed its mineralized top surface, and altogether continuous mineralization was indicated over an area of 500 by 200 yards. At present, two of the old floors having been permanently filled over, the galena horizon is seen only in one old floor, north-west of the pottery kilns, and in the top of the Thames Street quarry barely 100 yards east of the kilns. Both exposures yield wulfenite and radioactive asphaltite.

The top layer of the Magnesian Limestone is here a hard, light brown dolomite, from 1 to 3 inches in thickness, which breaks away from the somewhat softer dolomite below at a very thin clay parting. Its upper surface is compact and non-porous, but below this skin the rock is frequently fissured horizontally and composed of a porous mass of dolomite rhombs up to 1 mm. across. Galena occurs thinly disseminated through this granular dolomite, sometimes accompanied by minute crystals of cerussite, sometimes by wulfenite, and very rarely by traces of barytes and specks of malachite. Pyrite and blende are never visible in this layer, although they occur frequently in the deeper parts of the Thames Street quarry about 40 feet below this horizon, and there are no rhombohedral carbonates later than the rock-forming dolomite.

Here and there thin stringers of asphaltite are visible on the top surface of the dolomite, often in an irregular reticulate pattern (see fig. 1), but these extend downwards into the dolomite for only a few millimetres. Isolated specks and blebs of asphaltite also occur sparingly in the top 2 inches of the dolomite, some intimately associated with galena, others apparently free from it. The asphaltite is radioactive to a variable degree, but although hand specimens in a shielded geiger counter show moderate radioactivity, the asphaltite content of the layer is insufficient to allow of its detection with a field ratemeter.

The content of galena varies from mere traces to a few % at points only

a few inches apart, and so, to ascertain the average grade at this locality, one of the old weathering floors was sampled systematically to a depth of about 2 inches over an area of 1 500 square yards. Analysis of this average sample indicated 0·65 % Pb, 0·03 % MoO_3, 0·01 % Cu, trace Zn, very approximately 0·0005 % U_3O_8, and approximately 93 % carbonates (largely dolomite), 5 % quartz as rounded sand grains, a little

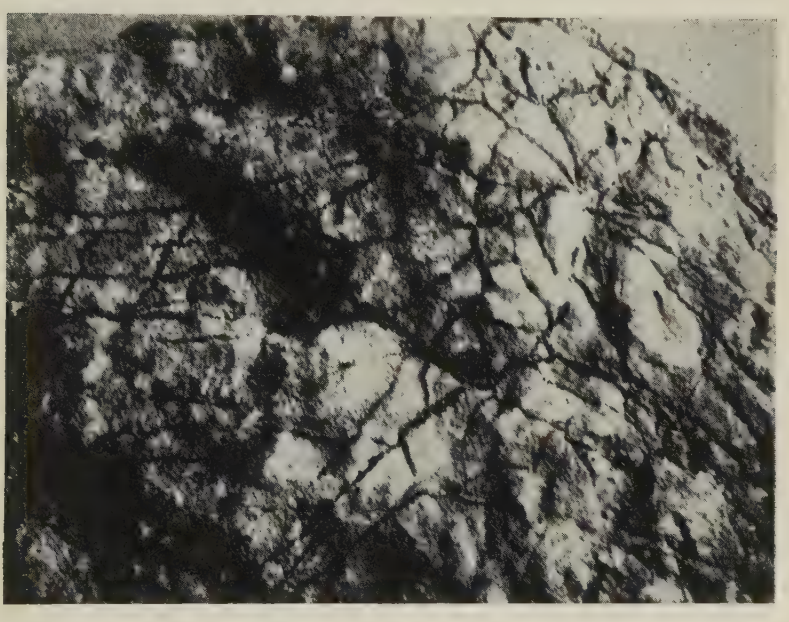

Fig. 1. Stringers of asphaltite on top surface of Lower Magnesian Limestone, Bulwell. Half natural size.

clay, and fractional percentages of asphaltite and barytes. The lead occurs very largely as galena, and cerussite is apparently a little more abundant than wulfenite.

About 1 mile north-east of the pottery the galena horizon was encountered at a depth of 20 feet in a water boring at Springfield (43/545463), and yielded rather coarse galena (up to 4 mm.), cerussite, a little wulfenite, and some asphaltite, all in reddish dolomite in the first 2 inches below the red Middle Marl.

Papplewick and Newstead. There are very poor exposures of the dolomite-marl contact in two overgrown quarries in this area, some 4 miles north of Bulwell. The first, a flooded quarry 500 yards north-west of Papplewick Hall (43/545520), has yielded galena, cerussite, chalcopy-

rite, and traces of malachite. The second, in Limekiln Wood, Newstead (43/536531), yielded galena, traces of wulfenite, and a little asphaltite.

Kirkby in Ashfield. At the northern end of Annesley long railway tunnel (43/504550), at the classic Permo-Triassic section described by Sherlock (1911, fig. 2, pp. 80 and 82), the top surface of the Lower Magnesian Limestone is now well exposed for a distance of 400 yards in broad benches along both sides of the cutting. The top layer of the dolomite is a dense fine-grained rock, but contains numerous very small cavities which may possibly be moulds of fossils. Galena is present only in traces, and would pass unnoticed unless carefully sought, but close inspection reveals frequent tiny spherules of malachite, small plates of wulfenite noticeable by their lustre, and occasional asphaltite.

Mansfield and Shirebrook. There are good exposures of the top of the Magnesian Limestone in the Mansfield White Stone quarries (43/534601), but usually it is not mineralized. In 1950, however, in one area, the top few inches consisted of a hard impervious dolomite cemented by white barytes and containing grains of black asphaltite, since found to be radioactive. Galena has not been seen here, but was recorded at this horizon 4 miles to the NNE. in Clipstone Colliery sinking at a depth of 385 feet (see Edwards, 1951, p. 157). Farther north, near Shirebrook, there are now few good exposures of this horizon, but in a railway cutting east of Shirebrook Station (43/536678) traces of asphaltite were seen.

Occurrences farther north. The occurrences in Yorkshire deserve brief mention here, as they indicate the wide distribution of galena and asphaltite at this horizon. Wulfenite is not yet known in this county. A little galena was seen in the top of the dolomite at a temporary exposure 500 yards ESE. of Woodsetts cross-roads (43/557836). This was the only exposure for many miles, but they become frequent to the south-west of Doncaster. Old workings at New Eddlington brickworks (43/531987) show the top of the dolomite with rather frequent stringers of radioactive asphaltite, rather less radioactive than at Bulwell, and much disseminated galena accompanied by calcite. The overlying marl, seamed with gypsum and containing marl pseudomorphs of halite hopper crystals, is feebly radioactive, but this may be largely due to the fact that it contains 5 % K_2O, like the Triassic marls described by Ponsford (1955, p. 40). Railway sections north of Warmsworth (44/543009) and at Sprotbrough (44/534017) as described by Mitchell (1947, p. 115) also show persistent galena below the Marl contact, usually with traces of asphaltite, and in the excavation of the Doncaster Bypass in 1959 similar occurrences were seen in Cusworth Park (44/542035).

Notes on the minerals.

Galena. The galena is largely disseminated through dolomite and is anhedral, but in cavities it has the common cubo-octahedral forms. Although the majority is unaltered, at several localities some of the crystals are corroded and may then have a sugary coating of cerussite crystals, the latter in a few cases encrusted by wulfenite, clearly indicating the sequence galena, cerussite, wulfenite. In concentrating these minerals it was noted that the galena was diamagnetic. Traces of copper minerals accompany the galena in Nottinghamshire, and in one case mineragraphic study revealed chalcopyrite intergrown with galena and later replacive covelline and chalcocite, but these features have yet to be studied in detail.

Spectrographic analyses of three samples of the galena were made by E. M. El Shazly in 1950 during a comparative study of trace elements in British sphalerites and galenas. These, like others from the Magnesian Limestone, were found to be characterized by much lower contents of antimony and silver than galenas from the Pennine ore deposits, as shown by the following figures recorded by El Shazly, Webb, and Williams (1957, p. 261):

Galena sample	Sb (*p.p.m.*)	Ag (*p.p.m.*)
Magnesian Limestone/Marl contact:		
Springfield, Bulwell (*a*)	10	10
,, ,, (*b*)	30	10
New Eddlington	20	15
Pennine Ore Deposits:		
Northern Pennines, average of 9	510	65
Derbyshire, average* of 4	200	25
Mill Close Mine, Darley Dale	100	10
Stars Wood, Ashover	10	5

* Including Mill Close Mine and Stars Wood.

While the contrast with the Pennine averages is very marked, the Derbyshire samples include some, the last two listed above, rather similar to those from the Magnesian Limestone. Of the other trace elements detected, Ba, Sr, Ti, and V are probably largely present in contaminating dolomite and marl, and Cu in sulphides; these do not call for comment, but it is of interest to note that 30 p.p.m. Mo were recorded in Bulwell galena (*a*), presumably from a trace of wulfenite, and that this was the only case in which molybdenum was detected in the seventy-seven British galenas examined.

Cerussite. The crystals are very small, colourless, grey, or white, and

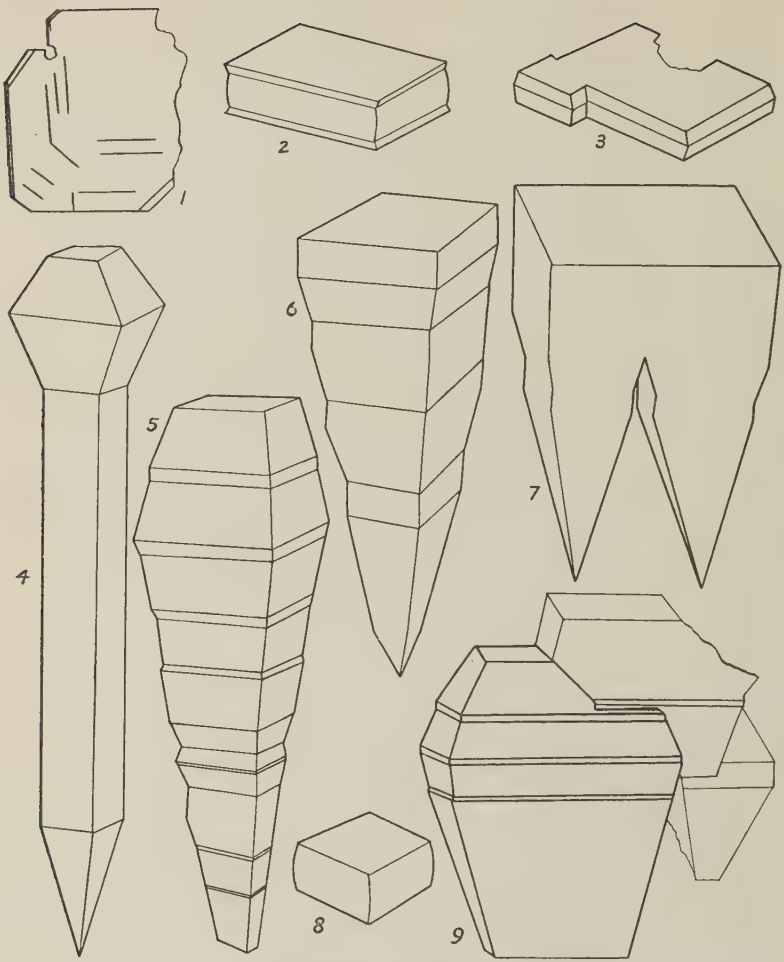

FIG. 2. Sketches of wulfenite crystals from Nottinghamshire. No. 1, Kirkby in Ashfield. Nos. 2–9, Bulwell.

No.	1	2	3	4	5	6	7	8	9
Size in mm. ...	1	0·3	1	0·6	0·4	0·25	0·45	0·5	0·4

often twinned. It is nearly always closely associated with galena, whereas the wulfenite frequently occurs quite independently of the sulphide. Rarely wulfenite coats cerussite, and the converse has not been observed.

Wulfenite. Although small, the wulfenite crystals display a variety of habits comparable in many ways with those from Struy, Inverness, described by Russell (1946), and from the classic Carinthian localities.

Platy crystals, the only type previously known from English localities, are common, often paper-thin and cream, buff, or pale greenish yellow in colour. Being basal plates they show perfect uniaxial negative optic axis figures. Thicker bevelled plates, up to $1\frac{1}{2}$ mm. across, colourless and transparent with adamantine lustre, occur at Kirkby in Ashfield (fig. 2, no. 1). At Bulwell pyramidal and prismatic forms (usually multiple combinations of both) are plentiful. These crystals are always pale, often of the same cream or buff colour as the dolomite on which they lie, and as they frequently show little lustre they are easily overlooked. A test with a dilute solution of sodium sulphide, which instantly stains the wulfenite black, is very effective in revealing these dull crystals. Although too small for angular measurements the forms appear to be the common ones, the prism {010}, pyramids {011} and {021} (in the setting adopted in Dana's System, 7th edn), and base {001}. Many small crystals at first sight appear to be simple pyramids more acute than {021}, but at high magnification are seen to be oscillatory combinations of {021} and {010}. The tapered combinations (fig. 2, nos. 5 and 6) are very reminiscent of Sir Arthur Russell's figured crystals from Struy, and the tooth-like combination (fig. 2, no. 7) of two parallel pyramids {011} terminating in a single prism {010} also matches one he describes from that locality (Russell, 1946, p. 151). The bipyramidal group, fig. 2, no. 9, is pale honey-yellow and transparent. A few squat and slightly curved prismatic crystals occur, and occasionally there are acicular prismatic crystals terminated by pyramids (fig. 2, no. 4) rather similar to some described by Schroll (1950) from Dirstentritt, Tyrol. The wulfenite is clearly the youngest mineral present in these rocks, and from its appearance might well be of very recent formation.

Uraniferous Asphaltite. This mineral occurs as small globular granules, or irregular blebs, or as narrow veinlets, dull black when weathered, but shiny black with conchoidal fracture and vitreous lustre when freshly broken. It is brittle, hardness lies between 2 and 3, the streak is black, and its density about 1·7. It is infusible in a Bunsen flame, and insoluble in common organic solvents. In polished section no organic structures are seen and it is clear that it is asphaltic in origin and not coalified plant tissue. The granules in some specimens from Mansfield are deeply cracked, as though by shrinkage.

From specimens from Bulwell Pottery a sample of the asphaltite was gouged out and hand picked as fragments 1 to 5 mm. across. This coarse concentrate was impure, and was therefore crushed to pass a 200-mesh sieve (75 μ openings) and centrifuged first in ethylene dibromide (sp.gr.

2·18), when galena and dolomite sank and were removed, and secondly in carbon tetrachloride (sp.gr. 1·58) in which the asphaltite sank, except for a mere trace of lighter material. The chemical composition of the inorganic constituents of the asphaltite fraction were first ascertained qualitatively by X-ray fluorescence analysis (kindly made by Dr. A. J. E. Welch), which indicated the presence of Pb, U, and Fe, minor amounts of Cu, Ni, Zn, and Mn, but no evidence of Th, Mo, or V. Mr. R. Pickup then provided the following quantitative chemical analysis: total ash content 18·91 %, including U_3O_8 0·89, PbO 3·90, Fe_2O_3,Al_2O_3 1·72, CaO 8·08, MgO 1·32 %. Traces of Cu, Zn, Mn, and Ti were also detected.

Examination of a polished section of the asphaltite showed that in addition to sparse coarse inclusions of dolomite and galena (veined and rimmed with minor amounts of covelline), there are numerous fine inclusions from 1 to 50 μ across which must have been included in the asphaltite analysed. These inclusions consist of carbonates, galena, and numerous euhedra of pyrite, 2 to 10 μ across, sometimes replaced by hematite, but as yet no uranium minerals have been detected. X-ray powder photographs of the analysed asphaltite show a broad diffraction band in the region 4·5 Å., characteristic of amorphous hydrocarbons, and also faint lines among which can be recognized the strongest lines of galena and calcite. It is evident, therefore, that the 'ash' is largely derived from calcite, dolomite, and galena, but the manner in which the uranium occurs is still unresolved and needs further study. Provisionally it is suggested that this uraniferous asphaltite is probably akin to the thucholite complexes from older formations, as described by Davidson and Bowie (1951). It differs considerably from the various hydrocarbons and 'carbonites' found in the Derbyshire mineral veins which are far less radioactive and are interpreted by Mueller (1954) as products of hydrothermal distillation.

Radiometric assays show that the uranium content of the asphaltite varies considerably from sample to sample and place to place. Observed values are a range from about 0·5 to 1·1 % U_3O_8 at Bulwell, 0·25 % at Mansfield, and 0·3 % at Eddlington, Yorks. As yet there is no evidence of radioactivity in this horizon other than that associated with the asphaltite. Various heavy mineral fractions, for example, showed negligible radioactivity unless contaminated with asphaltite. The overall radioactivity of the horizon appears to be too low to be detected at outcrop with a portable ratemeter, partly because the average uranium content is extremely low, partly because of the relatively high potash content of the overlying marl (around 5 % K_2O).

Comments on the ages and origins of the minerals.

The location of this varied assemblage of minerals at this contact horizon has presumably resulted from the trapping of metalliferous solutions beneath the semi-permeable Middle Marl. Deposition occurred in at least three stages, firstly galena, then asphaltite, and finally cerussite followed by wulfenite. The galena, introduced into the dolomite after the deposition of the Middle Marl, perhaps very soon after (diagenetically perhaps), or possibly much later, must be late Permian or younger in age, and as the Derbyshire lead mineralization post-dates the dolomitization of the Carboniferous Limestone by solutions descending from the Magnesian Limestone (see Dunham, 1952, p. 415), the geological evidence suggests the possibility of a common age for both types of galena occurrence, despite their stratigraphic separation.

Dr. S. Moorbath of the Department of Geology, Oxford University, has made lead isotope analyses of a sample of the Bulwell galena, and finds it yields a model age of 200 ± 60 million years, which by current time-scales corresponds to a Permo-Triassic origin. This dating is not inconsistent with the geological evidence, but publication of further details regarding this and other British galenas must be awaited before its true significance can be assessed.

Regarding the origin of the galena in this Upper Permian horizon, there appear to be two main alternatives. Firstly, to regard it as derived from the same sources as the galena of the Derbyshire lead deposits, and of similar hydrothermal origin, although presumably deposited at lower temperatures at this higher stratigraphic level. Or secondly, to consider it as resulting from redeposition of some of the syngenetic lead that was precipitated in certain phases of Zechstein sedimentation (see Deans, 1950), but which was subject to redistribution during the complex processes of dolomitization which ensued. In this case, which the writer tends to favour, the source of the lead might either be referred to hydrothermal springs discharging into the Zechstein sea (Dunham, 1952, p. 422), or to the intense cycle of weathering and chemical sedimentation of Zechstein times. A remarkable peculiarity of this horizon is the apparent absence of zinc, for in the Magnesian Limestone as a whole lead and zinc appear to be present in rather similar amounts.

The asphaltite is younger than the galena, which it frequently encloses, but how much younger is not at all clear. Some uraniferous hydrocarbons appear to originate by adsorption of heavy metals (U, V, Cu, Ni, &c.) by the hydrocarbon, whereas others are believed to result from the polymerization of light hydrocarbons (gas or oil) about radioactive

particles. The latter process seems the more probable in the present case, for the uranium is not accompanied by comparable amounts of vanadium or other adsorbed metals, and the asphaltite appears to be more akin to thucholite complexes than to the coaly complexes with adsorbed uranium such as Ponsford (1955, p. 40) has described from Gloucestershire. Provisionally it might be suggested that minute quantities of some uranium mineral were deposited in the dolomite at this contact and subsequently polymerized gas or oil as it was impounded beneath the Marl. Oilfields lie only a few miles to the east, so there is no difficulty in invoking migrating oil or gas in the small quantities sufficient to provide this asphaltite. The source of the uranium is obscure, but minor amounts of this element appear to be rather persistent in the Carboniferous rocks of this region, being recorded in phosphatic marine beds in the Nottingham–Derby coalfield, in Millstone Grit shales near Matlock, and in bituminous limestone near Castleton (Ponsford, 1955, pp. 31–34).

The cerussite and wulfenite are clearly secondary minerals, and in considering their origin one can be guided by the extensive literature on the Alpine lead–zinc–molybdenum deposits of Carinthia and the Bavaria–Tyrol border region, especially by the more recent papers of Hegemann (1949), Schroll (1953 *a* and *b*), and Meixner (1956). These classic wulfenite occurrences are widespread in a Middle Triassic dolomite formation (the Wettersteinkalk), but restricted to the oxidation zone of lead–zinc deposits. The primary lead–zinc sulphide ores are free from molybdenum, the latter only appearing later than galena, first as jordisite (colloidal MoS_2), which may alter to soluble ilsemannite or be partially transformed to microcrystalline molybdenite. Later, in the oxidation zone, cerussite develops, followed by wulfenite. The formation of wulfenite is ascribed to fixation in the secondary lead deposits of molybdenum derived from overlying bituminous dolomites and shales of the Trias, especially from a bituminous oolitic dolomite in the Cardita beds, which carries 50 to 400 p.p.m. Mo. In some cases wulfenite has formed in mines during the present century. The Nottinghamshire wulfenite occurrences have much in common with those of the Alps, e.g. paragenetic sequence, low silver and antimony contents of the galenas, absence of pyromorphite, &c., which suggests that the wulfenite may well be of similar origin. As yet, however, evidence of an adequate source of molybdenum in the Nottingham area is rather elusive. The Lower Lias of the Vale of Belvoir presumably carries appreciable molybdenum, for it gives rise to teart pastures, and traces

of molybdenite in the Mountsorrel granodiorite are well known, but connexions with these occurrences, which are at least 15 to 20 miles distant, seem dubious. Recent analyses of two samples from closer possible source beds, the Middle Marl from Bulwell Pottery and Lower Rhaetic black shales from Owthorpe (south-east of Nottingham), showed only 6 and 11 p.p.m. Mo respectively, which again seem hardly adequate. There remains the possibility, however, that the molybdenum derives from Permian or Triassic sediments, for the Marl Slate of Durham carries high concentrations of that element (Deans, 1950, p. 348); the recent formation of ilsemannite in the Magnesian Limestone at Billingham described by Raymond (1959), and the extent of the present wulfenite occurrences, also point to such an association. Some of the Bulwell wulfenite crystals appear as though they might be of very recent origin, and this possibility is strengthened by the evidence that molybdenum is still mobile in the Magnesian Limestone at Billingham, and in the Triassic dolomites of the Alps.

Acknowledgements. The writer is grateful to the owners of quarries and to British Railways for access to exposures, and to staff of the Geological Survey of Great Britain and the National Coal Board for much information and advice. Valuable help has also been received from colleagues in the Mineral Resources Division, Overseas Geological Surveys, and friends in the Universities.

References.

Davidson (C. F.) and Bowie (S. H. U.), 1951. Bull. Geol. Surv. Great Britain, no. 3, p. 1.

Deans (T.), 1950. Rept. 18th Internat. Geol. Congr., London, 1948, pt. vii, p. 340.

Dunham (K. C.), 1952. Trans. Geol. Soc. Glasgow, vol. 21, p. 395.

Edwards (W.), 1951. The Concealed Coalfield of Yorkshire and Nottinghamshire. Mem. Geol. Surv.

El Shazly (E. M.), Webb (J. S.), and Williams (D.), 1957. Trans. Inst. Mining Met., vol. 66, p. 241.

Hegemann (F.), 1949. Heidelberger Beitr. Min. Petr., vol. 1, p. 690.

Meixner (H.), 1956. Der Karinthin, Folge 31–32, p. 133.

Mitchell (G. H.) *et al.*, 1947. Geology of the Country around Barnsley. Mem. Geol. Surv.

Mueller (G.), 1954. Compt. Rend. XIX^{e} Congr. Géol. Internat., Alger, 1952, fasc. xii, p. 279.

Ponsford (D. R. A.), 1955. Bull. Geol. Surv. Great Britain, no. 10, p. 24.

Raymond (L. R.), 1959. Min. Mag., vol. 32, p. 172.

Russell (A.), 1946. Ibid., vol. 27, p. 151.

Schroll (E.), 1950. Tschermaks Min. Petr. Mitt., ser. 3, vol. 1, p. 325.

—— 1953*a*. Mitt. Österreich. Min. Gesell., Sonderheft 2, 60 pp.

—— 1953*b*. Carinthia II, 143 Jahrg., p. 47.

Sherlock (R. L.), 1911. Quart. Journ. Geol. Soc., vol. 67, p. 75.

Ages of some uranium and thorium minerals from East and Central Africa.

By A. G. Darnley, M.A., Ph.D., A.M.I.M.M., F.G.S., and J. E. T. Horne, M.A., F.G.S., Atomic Energy Division, Geological Survey of Great Britain,

G. H. Smith and T. R. D. Chandler, National Chemical Laboratory, Teddington, Middlesex,

and

D. F. Dance and E. R. Preece, Atomic Energy Research Establishment, Harwell, Berkshire.

[Read 3 November 1960.]

Summary. The following ages determined by the complete lead method have been accepted for minerals from a number of localities: uraninite, Nkana, Northern Rhodesia, 522 ± 15 m.y.; brannerite, Kansanshi, Northern Rhodesia, 503 ± 15 m.y.; uraninite, Shinkolobwe, Katanga, 642 ± 20 m.y.; davidite, Mavuzi, Mozambique, 578 ± 15 m.y.; monazite, Monkey Bay, Nyasaland, 597 ± 25 m.y.; samarskite, north-west Kenya, 635 ± 25 m.y. The significance of the results is briefly considered.

THIS is the second of a series of papers presenting age determinations on uranium and thorium minerals.[1] An explanation was given in the first paper (Darnley, Smith, Chandler, and Dance, 1960) of the errors taken into account in estimating the accuracy of the apparent ages provided by the different ratios. As these apparent ages seldom agree exactly it is sometimes difficult to decide what value to accept as the most probable age. No one ratio can be relied on to give the true age in all cases. Rather the evidence must be weighed for each specimen or group of specimens, and cognizance taken of the geological and mineralogical environment. Because factors causing discordance may affect different specimens from the same locality to different extents, it is a great advantage to have results from two or more specimens. In this paper certain apparent ages have been rejected either because of their discordance or because they are based on only very small amounts

[1] Preliminary accounts with slightly different ages were issued on a limited circulation by the Atomic Energy Division, Geological Survey of Great Britain, as Age Determination Reports Nos. 3, 7, 8, 9, 12, and 14.

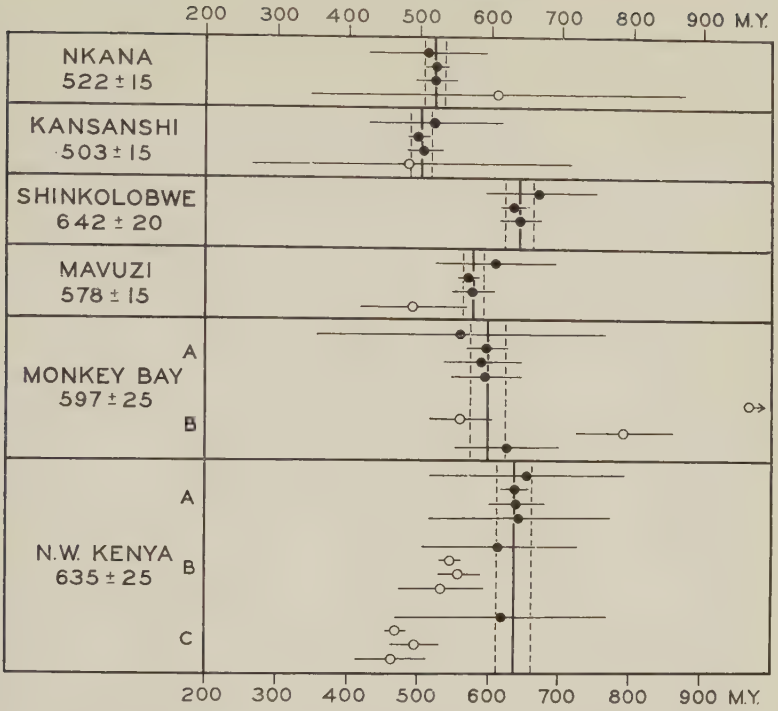

FIG. 1. Graphical summary of the results. For each specimen the apparent ages are plotted from top to bottom in the order 207/206, 206/238, 207/235, 208/232. The horizontal lines represent the estimated errors. Apparent ages shown by open circles have been rejected for the reasons stated in the text. The weighted mean of the remaining apparent ages is accepted as the age of each specimen or group of specimens. It is indicated by a vertical line. The error derived for the accepted age is shown by broken lines.

of lead-208 and thorium. The accepted age for each specimen or group is taken as the mean of the remaining apparent ages weighted in inverse proportion to their estimated errors. An approximate measure of the error of the accepted age is taken as the weighted mean of the individual estimated errors divided by the square root of the number of apparent ages involved. To facilitate appraisal of the results, they are presented graphically in fig. 1.

Uraninite from Nkana, Northern Rhodesia.

The uraninite used for this determination was derived from a concentrate provided by Dr. T. D. Guernsey of Rhokana Corporation Ltd. The

original concentrate was taken from a mass of fractured and recemented uraninite, amounting to several cubic inches, collected from the Mindola Section of Nkana mine. This mode of occurrence is not typical of the disseminated uraninite–brannerite mineralization at Nkana.

The uraninite is fresh and entirely free from secondary uranium minerals, and from galena. In an uncrushed specimen, melonite ($NiTe_2$) is a prominent accessory mineral together with lesser amounts of bornite, chalcopyrite, digenite, and chalcocite. The opaque minerals are set in a ground-mass of calcite, quartz, biotite, chlorite, and albite. The original concentrate was purified electromagnetically to remove the small quantity of accessory minerals present.

TABLE I. Nkana uraninite.

Chem. anal. (*wt.* %)	*Lead-isotope proportions*			*Isotopic ages* (*m.y.*)
	Uraninite	*Galena**	*Uraninite corrected*	
Pb 5·79	^{204}Pb 0·0099±0·0004	1	—	207/206 512±85
U 75·82$_1$	^{206}Pb 94·02±0·05	18·25	93·84	206/238 524±15
Th 0·14$_1$	^{207}Pb 5·53±0·05	15·88	5·37	207/235 522±30
	^{208}Pb 0·446±0·004	38·47	0·065	208/232 610±265

* The isotopic proportions of common lead used throughout the paper are based on the average of 10 galena analyses from Katanga and Northern Rhodesia. Nine are taken from Holmes and Cahen (1956, 155–6) and one is a new analysis of galena from Broken Hill (204:206:207:208 = 1:18·08:15·89:39·07).

The chemical and isotopic analyses and the apparent ages derived from them are given in table I.

Discussion. There is good agreement between the ages derived from the first three ratios, on which the accepted age of 522±15 m.y. is based. The small amount of thorium present, coupled with the sensitivity of the 208/232 ratio to the common lead correction, makes the thorium age less reliable. Holmes and Cahen (1957) have reported another uraninite analysis from Nkana (mode of occurrence unknown) giving the following results: 207/206 612 m.y., 206/238 527 m.y., 207/235 540 m.y. They have accepted the 207/206 age as being most reliable, but in view of the discordance between the apparent ages, this must now be regarded as unsatisfactory. The association of melonite with uraninite is unusual, although small amounts of disseminated melonite have been seen in a few other specimens from Nkana. Melonite has also been recorded at Shinkolobwe (Derricks and Vaes, 1956).

Further work is in progress on material more typical of the disseminated mineralization at Nkana.

Brannerite from Kansanshi, Northern Rhodesia.

The specimen analysed was provided by Mr. C. J. McFarlane, manager of Kansanshi Copper Mining Co., Ltd. The mine is situated to the north-west of the Rhodesian Copper Belt at 12° 05′ S., 26° 25′ E. The specimen was collected at the point of intersection of A vein with B vein on the 290-foot level from the Main North Shaft. The mineral association of this particular specimen is not known, but in others from the

TABLE II. Kansanshi brannerite.

Chem. anal. (*wt.* %)	*Lead-isotope proportions*			*Isotopic ages* (*m.y.*)
	Brannerite	*Galena*	*Brannerite corrected*	
Pb 3·13	^{204}Pb 0·0029±0·0003	1	—	207/206 522±95
U 42·91$_0$	^{206}Pb 94·4±0·1	18·25	94·35	206/238 498±15
Th 0·072$_1$	^{207}Pb 5·47±0·04	15·88	5·42	207/235 507±25
	^{208}Pb 0·161±0·007	38·47	0·049	208/232 487±225

mine coarsely crystalline anhedral brannerite, in masses up to 5 cm. across, is associated with chalcopyrite and calcite in approximately equal proportions, and with minor pyrite.

The brannerite is massive in habit and unaltered; it is steely-black with a submetallic lustre. A powder photograph shows it to be essentially metamict. X-ray and optical spectrographic analyses show major uranium and titanium, with subordinate lead and yttrium. Also present are minor proportions of Ca, Zr, Fe, lanthanons (particularly Dy and Er), V, Sr, Mg, and Si. Examination of a polished section of the mineral shows minor amounts of galena, chalcopyrite, and rutile, together with traces of bornite. The even distribution of the minute specks of galena suggests it is derived from radiogenic lead and therefore no attempt was made to remove any of the inclusions prior to analysis. The analyses and calculated ages are given in table II.

Discussion. All four ages are reasonably concordant, although the agreement of the 208/232 age with the others must be regarded as somewhat fortuitous in view of the very small amount of thorium present. The weighted mean of the first three ages is 503±15 m.y., which compares closely with the age obtained for Nkana. These results support the view that uranium minerals in Northern Rhodesia were formed about 100 m.y. after those in Katanga.

Uraninite from Shinkolobwe, Katanga.

This analysis, carried out for the purposes of comparison with the Nkana uraninite, was made on a specimen of massive fresh uraninite from

Shinkolobwe, presented by the Union Minière du Haut Katanga. No concentration was required. The results are given in table III.

Discussion. Because of the low thorium and lead-204 contents of the analysed material, the common lead correction is based on the amount of lead-208 present. The results are concordant within the limits of error and the weighted mean of 642±20 m.y. is taken as the true age.

TABLE III. Shinkolobwe uraninite.

Chem. anal. (*wt.* %)	*Lead-isotope proportions* *Uraninite*	*Galena*	*Uraninite corrected*	*Isotopic ages* (*m.y.*)
Pb 7·15	^{204}Pb < 0·004	0·0259	—	207/206 671±80
U 76·73$_5$	^{206}Pb 94·03±0·04	0·4744	93·97	206/238 635±20
Th 0·014$_9$	^{207}Pb 5·83±0·03	0·4125	5·78	207/235 643±30
	^{208}Pb 0·13±0·01	1	—	

TABLE IV. Mavuzi davidite.

Chem. anal. (*wt.* %)	*Lead-isotope proportions.* *Davidite*	*Galena*	*Davidite corrected*	*Isotopic ages* (*m.y.*)
Pb 0·65	^{204}Pb 0·024±0·001	1	—	207/206 608±85
U 7·63$_2$	^{206}Pb 92·3±0·1	18·25	91·86	206/238 569±15
Th 0·28$_1$	^{207}Pb 5·87±0·03	15·88	5·49	207/235 576±30
	^{208}Pb 1·85±0·03	38·47	0·93	208/232 492±75

Davidite from Mavuzi, Tete, Mozambique.

The davidite used for this analysis was collected by Professor C. F. Davidson and Dr. J. A. E. Bennett in 1948. The locality is 30 miles north-west of Tete at 15° 50′ S., 33° 25′ E., where the mineral occurs in shear zones filled with scapolite and carbonate in pre-Karoo norites and anorthosites. Associated minerals include rutile, sphene, magnetite, ilmenite, apatite, tourmaline, molybdenite, pyrite, and chalcopyrite. A detailed account of the deposit is given by Davidson and Bennett (1950), and of the mineral itself by Bannister and Horne (1950).

The mineral is a metamict titanate of iron and uranium. X-ray spectrographic analysis shows subordinate lanthanum, cerium, chromium, and vanadium, with minor proportions of Pb, Sr, Y, Zr, Th, and Ca. Freshly fractured surfaces are black with a bright submetallic to vitreous lustre and fragments bounded entirely by such surfaces were available for analysis (table IV).

Discussion. The first three ages are in fair agreement and give a weighted mean of 578±15 m.y., which is accepted as the most probable

age. The thorium–lead age is less satisfactory. Since approximately 50 % of the lead-208 present in the specimen is attributable to common lead, this age is particularly sensitive to the appropriateness of the lead-isotope proportions used for correction. The accepted age falls between that of the Rhodesian and the Katangan uranium occurrences. However, the age sequence suggests that there may have been some slight loss of radiogenic lead and another determination is in hand to check this possibility. It is interesting that Davidson and Bennett (1950) remark that 'the Mavuzi rocks show more widespread regional scapolitization than any other igneous complex known to the writers'. Extensive scapolitization is also characteristic of many basic and metasedimentary rocks in Northern Rhodesia, including the Copperbelt (Jackson, 1932; Darnley, 1960).

Monazite from Monkey Bay, Lake Nyasa, Nyasaland.

Monazite occurs as a minor constituent in ilmenite-rich sands that are found at the southern end of Lake Nyasa on the east side of the Cape Maclear Peninsula, 14° 15′ S., 35° 07′ E. They lie beside the road to Monkey Bay between 16 and 23 road miles north-west of Fort Johnston. The monazite-bearing sands are mostly in raised beaches approximately 30 feet above the present lake surface, but small areas have been found at intervening levels down to the present-day storm beach. The high-level beaches are consolidated by clayey material. Associated heavy minerals include magnetite, garnet, and zircon. As the source of the monazite has not been established, the geological significance of this determination is limited. It was in fact undertaken to give an indication of the possible source rocks. The results are of interest in demonstrating that detrital monazite is capable of yielding concordant ages.

Monazite was derived from two samples. One was collected by Mr. M. S. Garson of the Nyasaland Geological Survey, and the monazite subsequently concentrated by the Mineral Resources Division of the Overseas Geological Surveys using an electromagnetic separator and methylene iodide. The other was provided by Rhodesian Selection Trust Exploration Ltd. of Salisbury, Southern Rhodesia, and the monazite was concentrated electromagnetically at A.E.D. The analyses and derived ages are given in table V.

Discussion. The thorium–lead ages of both concentrates show good agreement. The lead–lead and uranium–lead ages of the first analysis agree well with the thorium–lead age, but this is not true in the case of the second. Both the 207/235 and 207/206 apparent ages are high. The

reason for this is not known. The analysed material was composed of clear, apparently unaltered grains, and the analytical results show that it was free from common-lead contamination. However, the first analysis indicates that the processes of weathering and transportation are not in themselves sufficient to produce discordant ages. The accepted age, which is the weighted mean of the four apparent ages derived from the first analysis and the 208/232 age from the second analysis, is 597 ± 25 m.y.

TABLE V. Monkey Bay monazite.

Chem. anal. (*wt.* %)	*Lead-isotope proportions*			*Isotopic age* (*m.y.*)
	Monazite	*Galena*	*Monazite corrected*	
Pb 0·185	^{204}Pb 0·111 ± 0·0008	1	—	207/206 559 ± 205
U 0·15$_3$	^{206}Pb 7·13 ± 0·04	18·25	6·95	206/238 597 ± 30
Th 6·41$_6$	^{207}Pb 0·581 ± 0·008	15·88	0·405	207/235 589 ± 55
	^{208}Pb 92·3 ± 0·1	38·47	91·9	208/232 594 ± 50
Pb 0·18	^{204}Pb > 0·002			207/206 1533 ± 160
U 0·17$_0$	^{206}Pb 7·34 ± 0·09	No correction required		206/238 558 ± 45
Th 5·95$_0$	^{207}Pb 0·69 ± 0·02			207/235 792 ± 70
	^{208}Pb 92·0 ± 0·1			208/232 625 ± 75

Samarskite from north-western Kenya.

The samarskite specimens were provided by Mr. H. Wreford Smith of Kitale, Kenya. They came from three separate pegmatites (Kokusan, Kenailmet, and Morukong) situated within a mile of each other at approximately 1° 59′ N., 35° 04′ E., in the Turkana Province. The pegmatites belong to a swarm striking approximately north–south, and cutting folded plagioclase amphibolites and limestones of the Basement System. Dr. G. J. H. McCall, formerly of the Kenya Geological Survey, reports in a personal communication that the feldspar present is often perthitic and is associated with pale green muscovite and occasionally biotite with vermiculite. Samarskite, columbite, garnet, and tourmaline are present together with some corundum.

The samarskite shows fresh black conchoidally fractured surfaces with a bright vitreous lustre. X-ray and optical spectrographic analyses of each specimen show them to be essentially niobates of uranium, yttrium, and iron, with subordinate tantalum, thorium, and lanthanons (particularly gadolinium, dysprosium, and samarium). Minor proportions of Ti, Pb, Mn, Zr, Ca, Si, and Al are also present. X-ray photographs of unheated specimens show they are metamict, but samarskite patterns are obtained on heating in nitrogen at 1 000° C.

Discussion. Results on material from Morukong are very satisfactory,

but there is internal discordance in the ages obtained on the specimens from Kenailmet and Kokusan. However, the 207/206 ages of all three specimens are similar. The pattern of discordance with 207/206 > 207/235 > 206/238 indicates that lead loss is the most likely cause of the

TABLE VI. Kenya samarskite.

Chem. anal. (*wt.* %)	*Lead-isotope proportions*			*Isotopic age* (*m.y.*)
	Samarskite	*Galena*	*Samarskite corrected*	
		Morukong.		
Pb 1·18	^{204}Pb 0·008±0·002	1	—	207/206 654±140
U 12·12$_7$	^{206}Pb 90·5±0·1	18·25	90·25	206/238 636±20
Th 1·49$_4$	^{207}Pb 5·64±0·13	15·88	5·51	207/235 639±40
	^{208}Pb 3·88±0·08	38·47	3·57	208/232 642±130
		Kenailmet.		
Pb 1·08	^{204}Pb 0·053±0·002		—	207/206 613±110
U 12·46$_6$	^{206}Pb 87·1±0·1	As above	86·13	206/238 544±15
Th 2·24$_1$	^{207}Pb 6·00±0·07		5·16	207/235 557±30
	^{208}Pb 6·86±0·06		4·82	208/232 531±60
		Kokusan.		
Pb 0·77	^{204}Pb 0·075±0·002		—	207/206 618±150
U 10·13$_4$	^{206}Pb 85·5±0·1	As above	84·13	206/238 468±15
Th 2·02$_1$	^{207}Pb 6·24±0·13		5·05	207/235 495±35
	^{208}Pb 8·18±0·08		5·29	208/232 462±50

discordances and the validity of this assumption can be demonstrated by calculating the percentage of radiogenic lead which must be added to the mineral to bring the 206/238 age into agreement with the 207/206. The 207/235 result will then automatically fall into line, as the three ratios are interdependent, but the 208/232 age will only agree if lead loss is in fact the predominant cause of the discordance.

The results tabulated below show that there is good agreement between the adjusted 206/238 and 208/232 ages:

	207/206	206/238 *adjusted*	% Pb *added*	208/232 *adjusted*
Kenailmet	613	613	13·4	601
Kokusan	618	618	33·4	614

It is concluded from the geological evidence that the three pegmatites are of the same age, and that the discordance in the Kenailmet and Kokusan results is due to lead loss. The weighted mean of the four Morukong ages and the 207/206 ages of Kenailmet and Kokusan is 635 m.y., which is taken as the most probable age with an error of ±25 m.y. The determination demonstrates the value of analysing at east two specimens if this is at all possible, as the Kenailmet or Kokusan

results alone might have been misleading or their correct interpretation lacking in conviction. Mica specimens collected from the Kenailmet pegmatite by Dr. McCall have been submitted to the Department of Geology and Mineralogy at Oxford for age determination by the potassium argon and rubidium–strontium methods. These results will be of interest for comparison with the lead age accepted here.

References.

Bannister (F. A.) and Horne (J. E. T.), 1950. Min. Mag., vol. 29, p. 101.

Darnley (A. G.), 1960. Trans. Inst. Min. Metall., vol. 69, p. 137.

—— Smith (G. H.), Chandler (T. R. D.), Dance (D. F.), and Preece (E. R.), 1960. Min. Mag., vol. 32, p. 654.

Davidson (C. F.) and Bennett (J. A. E.), 1950. Ibid., vol. 29, p. 291.

Derriks (J. J.) and Vaes (J. F.), 1956. Proc. 1st Int. U.N. Conf. Peaceful Uses of Atomic Energy, Geneva, 1955, vol. 6, p. 94.

Holmes (A.) and Cahen (L.), 1957. Géochronologie africaine 1956. Mém. Acad. R. Sci. colon. Cl. Sci. nat., new series, vol. 5, no. 1, 169 pp.

Jackson (G. C. A.), 1932. Quart. Journ. geol. Soc., vol. 88, p. 443.

Amphibolite–granulite facies assemblages in southern Nyasaland.

By S. W. Morel, B.Sc., Ph.D.

67 The Rise, Sevenoaks, Kent

[Taken as read, 26 January 1961.]

Summary. The mineral assemblages developed in a variety of high-grade metamorphic rocks from southern Nyasaland are compared with standard metamorphic facies mineral assemblages proposed by some authors.

THE Middle Shire area of Nyasaland lies roughly midway between the southern tip of Lake Nyasa and the Zambezi river. It includes the western side of the Shire Highlands horst, the central section of the Shire rift, and the eastern face of the Kirk mountains scarp which here forms the watershed between the Nyasa and Zambezi troughs.

This area is occupied mainly by high-grade gneisses and granulites of the Mozambique Belt, which prior to their metamorphism were intruded by a series of pre-Cambrian plutonic rocks ranging from ultrabasic to syenitic in composition.

The gneisses and granulites can be divided into two groups on the basis of metamorphic grade. In the eastern part of the area gneisses and granulites of charnockitic type are prevalent whilst in the central and western parts amphibolites and hornblende-biotite gneisses are common. Horizons of marble, calc-silicate granulite and arenaceous schist are common to both groups, as are highly metamorphosed basic and ultrabasic intrusives (Morel, 1955, 1958).

Facies delineation. During the geological mapping of the Middle Shire area it was found that the gneisses changed in texture from lepidoblastic to granulitic in what was later described as the transition zone between the amphibolite and granulite facies (Morel, 1958, fig. 1). Later petrographic work showed that this textural change was accompanied by several mineralogical changes: hypersthene appeared in the granulitic rocks; the oligoclase feldspar of the lepidoblastic gneisses was replaced by andesine in the granulitic rocks; pale green augite became very common in the granulites; the bluish-green hornblende of the hornblende-biotite gneisses and amphibolites was replaced by an olive-

green hornblende in the basic charnockitic granulites; sphene disappeared; and biotite became less common and foxy-red in colour.

As hornblende-biotite-gneisses are the commonest rock type found in the central and western parts of the Middle Shire area, and charnockitic

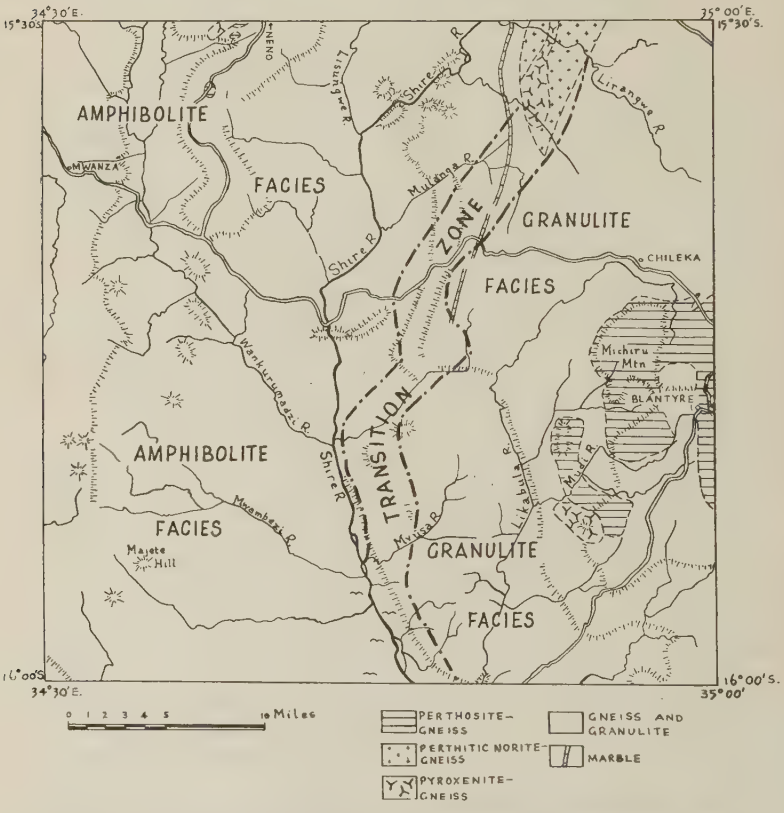

Fig. 1. Sketch map of the Middle Shire area showing metamorphic facies.

granulites form the country rocks of the eastern part, these two groups of rocks were utilized to delineate the boundaries between the amphibolite and granulite facies.

The assemblage hornblende–biotite–oligoclase was taken to be critical for the amphibolite facies and hypersthene–diopside–andesine as typical of the granulite facies (Turner and Verhoogen, 1951, p. 446).

It was found that a broad transition zone, up to two miles in width,

was present in which assemblages common to both groups obtained. To the west of this transition zone hypersthene is rare and sphene is common, whilst to the east the reverse holds and sphene is only found in calc-silicate rocks (fig. 1).

Once the boundaries of the transition zone had been determined on the basis of the above assemblages it became possible to compare the mineral parageneses of the less abundant rock types with the standard assemblages as presented by Turner and Verhoogen (1951) and Ramberg (1952).

Amongst psammitic granulites it was found that muscovite occurs partially altered to sillimanite some seven to eight miles to the west of the transition zone. Ramberg (1952, p. 158) states that the muscovite→sillimanite reaction occurs abruptly at the amphibolite–granulite facies boundary. The evidence quoted above suggests that this reaction may take place before the appearance of hypersthene in rocks of appropriate composition that are undergoing increasing metamorphism.

In the magnesia-rich ultrabasic rocks the break-up of biotite to form orthoclase and anthophyllite has been detected in biotitites that lie a mile or more to the west of the transition zone. This reaction would appear to represent a stage in the reaction: Mg-phlogopite + silica → enstatite + orthoclase, which Ramberg (1952, p. 159) indicates as taking place at the boundary between the amphibolite and granulite facies. The metamorphosed ultrabasic intrusions are mainly biotitites and biotite-pyroxenites in the western and central parts of the Middle Shire area, whilst to the east, amongst the charnockitic rocks, they are largely websterites, and it appears likely that this difference may be a function of their metamorphic grade.

Calc-silicate Granulites. As the main mineral groups taking part in reactions at the amphibolite–granulite facies boundary are almost entirely members of mix-crystal series, it is not to be expected that this boundary can be represented on a geological map by other than a relatively broad transition zone. In view of this supposition it is of interest to compare the zonal relationships amongst calc-silicate granulites that Kennedy (1949, pp. 43–56) has described from the Scottish Highlands with those of southern Nyasaland.

Kennedy succeeded in delineating zonal relationships between members of the Moine Series to within a few hundred feet by using certain mineral assemblages that are present amongst the pelitic and arenaceous granulites of the Morar–Sunart area. He divided the accompanying calc-silicate rocks into four classes, which he correlated with Eskola's

facies as shown in table I, where a correlation with the Middle Shire facies is also put forward.

Kennedy thought that the Scottish rocks belonged to a single isochemical series in which variations in chemical composition were due to changes brought about in the attainment of mineralogical equilibrium during the process of metamorphism.

TABLE I.

Eskola's facies	*Kennedy's facies*	*Middle Shire facies*
Epidote–amphibolite	*Group* 1. Quartz–calcite–zoisite–acid-plagioclase–hornblende–garnet	Absent
	Group 2. Quartz–zoisite–acid-plagioclase–hornblende–garnet	Absent
Amphibolite	*Group* 3. Quartz–bytownite–hornblende–garnet	Epidote–hornblende–calcic-plagioclase
Pyroxene hornfels	*Group* 4. Quartz–bytownite–pyroxene–garnet	*Granulite facies* Hedenbergite–calcic-plagioclase–calcite–garnet

The petrology of the Nyasaland calc-silicate granulites has been described elsewhere (Morel, 1958, pp. 26–29) and it is unlikely that these rocks represent an isochemical series, for they are strongly banded into alternating layers rich in pyroxene or garnet, which vary from a few millimetres to several centimetres in thickness. This banding appears to be due to compositional differences between the layers of the parent sediment.

The garnet of the Scottish rocks is found in each of Kennedy's groups but in Nyasaland this mineral is restricted to the upper part of the amphibolite facies and the granulite facies, where it appears to be replacing hedenbergite (Morel, 1958, fig. 5B). The garnet of the Nyasaland rocks is probably an andradite-grossular.

The pyroxene of the Scottish rocks is a colourless and apparently highly aluminous augite. That of Nyasaland is a deep emerald hedenbergite with strong pleochroism. In the amphibolite facies its place is taken by hornblende, in agreement with Kennedy's findings, but, considering their different compositions, it is unlikely that the two pyroxenes and their accompanying feldspars crystallized under strictly comparable conditions.

In the Middle Shire area epidote is common in the calc-silicate granulites of the amphibolite facies and the transition zone whilst Kennedy

did not find it in rocks whose metamorphic grade exceeded that of the epidote-amphibolite facies. When calcite is present in the Nyasaland examples it is frequently accompanied by primary scapolite of a mizzonitic composition.

In a later paper von Knorring and Kennedy (1958) discussed the mineral paragenesis and metamorphic status of a garnet-hornblende–pyroxene–scapolite gneiss from the Shai Hills, Ghana. They published two chemical analyses of these rocks and stated that these indicate that they were formed from basic igneous rocks, and are comparable to some eclogite rocks. They considered that the petrographical uniformity of the formation and the absence of relict banding provide an indication of an original igneous character, and that these rocks formed under conditions transitional between those of the amphibolite and eclogite facies. They reached this conclusion from the association of hornblende and plagioclase with garnets and pyroxenes of eclogitic type in the Shai Hills rocks. Because of differences in mineral chemistry they did not assign these rocks to Turner's almandine–diopside–hornblende subfacies of the amphibolite facies (Turner and Verhoogen 1951, p. 458), and proposed an association garnet pyroxene hornblende, which they consider to be transitional between the amphibolite and eclogite facies, and to be chemically distinct from the almandine–diopside hornblende subfacies.

From the point of view of facies delineation in the field it would be impractical to differentiate between the garnet pyroxene–hornblende assemblage and Turner's almandine–diopside hornblende subfacies, since chemical analyses are required to detect the jadeite component of the pyroxene.

In the Ncheu area of Nyasaland (Morel, 1956) garnet-hornblende–diopside gneisses are commonly interlayered with hypersthene-bearing charnockitic granulites. In this case there can be no difference in metamorphic grade between the two rock types, and the differing mineral parageneses can only represent original compositional differences. Howie and Subramaniam (1957, p. 582) have shown that the presence or absence of garnet is controlled only by the chemical composition of the rock.

It is apparent that the almandine–diopside–hornblende subfacies of the amphibolite facies overlaps into the granulite facies and one may ask whether any useful purpose will be served by further subdivisions of the imprecise but useful facies concept until more is known about the mineral parageneses of rocks of differing chemical compositions that have undergone the same degree of metamorphism.

Acknowledgement. The fieldwork upon which part of this paper is based was carried out whilst the writer was employed by the Nyasaland Government. The opinions expressed are those of the writer and not necessarily those of the Nyasaland Geological Survey.

References.

Howie (R. A.) and Subramaniam (A. P.), 1957. Min. Mag., vol. 31, p. 565.
Kennedy (W. Q.), 1949. Geol. Mag., vol. 86, p. 43.
Morel (S. W.), 1955. Ibid., vol. 92, p. 241.
—— 1956. The geology of the Ncheu area. Rept. Geo. Surv. Nyasaland (unpubl.).
—— 1958. The geology of the Middle Shire area. Bull. Geol. Surv. Nyasaland, no. 10.
Ramberg (H.), 1952. The origin of metamorphic and metasomatic rocks. Chicago (Chicago Univ. Press).
Turner (F. J.) and Verhoogen (J.), 1951. Igneous and metamorphic petrology. New York (McGraw-Hill).
von Knorring (O.) and Kennedy (W. Q.), 1958. Min. Mag. vol. 31, p. 846.

On the lithium amphibole holmquistite, from Benson pegmatite mine, Mtoko, Southern Rhodesia.

By O. von Knorring, Ph.D., M.Sc., and G. Hornung, B.Sc., F.G.S.

Research Institute of African Geology, Department of Geology, the University of Leeds.

[Taken as read 26 January 1961.]

Summary. A new occurrence of holmquistite is described. The mineral is found in amphibolite at the contact of a lithium pegmatite. Chemical analyses and optical data of the holmquistite and an associated hornblende are given.

Osann (1913) defined holmquistite as a monoclinic lithium-glaucophane, and this interpretation was retained by Sundius (1946, 1947) in his classification of the hornblendes, although with some reservations. Machatschki (1953) grouped holmquistite with the clino-amphibole grunerite–cummingtonite and regarded it as a lithium amphibole analogous to the lithium pyroxene spodumene.

On the basis of X-ray studies, Ginzburg *et al.* (1958) and Vogt *et al.* (1958) have shown that holmquistite is not monoclinic, but is an orthorhombic amphibole akin to anthophyllite in structure, whose formula can be derived from the latter by the substitution of LiAl for MgMg. The lattice constants of these minerals according to Vogt *et al.* are: holmquistite a 18·36, b 17·75, c 5·29 Å., anthophyllite a 18·56, b 18·08, c 5·28.

In addition to the original find of holmquistite from the Utö spodumene pegmatite near Stockholm by Osann, holmquistite has been recorded by Palache *et al.* (1930) from the hiddenite (a green, gem variety of spodumene) deposit in Alexander County, North Carolina, by Ginzburg and Ginzburg (1950) from spodumene pegmatites in the northern Kola Peninsula, and by Karpoff (1960) from lithium-rich pegmatites in Lacorne area, Province of Quebec. In all these occurrences holmquistite has been found developed in the country rock, of variable composition, close to the contact of spodumene-bearing pegmatites, and in all cases the origin of the lithium amphibole has been attributed to lithium metasomatism.

The present holmquistite was found by one of us (G. H.) on the Benson claims during an investigation of pegmatites in the Mtoko–Fungwe area

in the north-eastern part of Southern Rhodesia. Here a narrow, arcuate belt of metasediments and metavolcanic rocks of Bulawayan (Precambrian) age, bounded and in part interrupted by granite and granite-gneiss, extends across the Mtoko and Fungwe Reserves. Protruding through the belt in the Mtoko Reserve is the granite mass of Bangawia, which forms a major pegmatite focus immediately adjacent to the Benson claims (17° 2′ S., 32° 15′ E.).

The Benson lithium pegmatites are the most important in this part of Rhodesia, and display a unique assemblage of economic minerals: amblygonite, spodumene, lepidolite, beryl (white, green, pink, and orange), pollucite, bismutite, cassiterite, microlite (with a wide colour range), columbite-tantalite, manganotantalite, stibiotantalite, and simpsonite.

In the main holmquistite occurrence at Benson 1, the marginal zone of the amphibolite has been transformed into a holmquistite-bearing rock extending over an area of at least 80 by 20 feet, around the folded extremity of a spodumene lepidolite pegmatite. At the contact there is a selvage rich in a biotite containing lithium and fluorine together with feldspar, fluorite, and apatite; followed by a zone consisting of hornblende, holmquistite, biotite, feldspar, quartz, and sphene; and finally a dominantly holmquistite-bearing rock composed of 43 % holmquistite, 13 % hornblende, 2 % ore, 1 % biotite, 1 % clino-zoisite, and 40 % of mainly quartz and some feldspar.

In hand specimen the holmquistite rock is bluish grey in colour and consists predominantly of an extremely thin fibrous mineral, although, with the naked eye, the presence of holmquistite is not at first apparent. With a strong hand lens, however, the characteristic jacaranda-blue colour of the holmquistite (resembling kyanite) is clearly visible. In thin-section the fibre-like crystals of the lithium amphibole are seen to be in parallel arrangement and appear to have crystallized later than the associated green hornblende. Partial replacement or pseudomorphs of holmquistite after hornblende, as recorded by Ginzburg and Ginzburg (1950), have as yet not been observed. The holmquistite fibres are up to 5 mm. in length and some tenths of a millimetre in width. Striated faces are observed on {110} and smooth faces on {100}. No terminal faces have been noticed.

Holmquistite exhibits a characteristic pleochroism: α pale yellow, β pink-violet, and γ pale purple. The associated hornblende is of common green colour with pleochroism: α straw-yellow, β pale green, and γ blue-green. Additional physical data of the two amphiboles are shown

in table I. An X-ray powder photograph of holmquistite from the Benson mine is given in fig. 1.

The contact of Benson 3 pegmatite reveals a more asbestiform variety of holmquistite in a lime-green clay rock, again outside a biotite-rich selvage. Benson 4 mine yields holmquistite in a similar clay rock, and also in a drag folded and sheared amphibolite. At present, the country rock marginal to 8 lithium pegmatites is known to contain holmquistite.

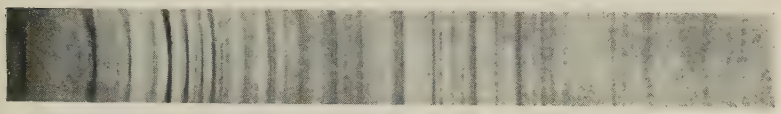

FIG. 1. X-ray powder photograph of holmquistite from Benson 1 pegmatite, Mtoko. 9 cm. camera, Fe-$K\alpha$ radiation.

Sundius (1959) points out that the rhombic character of holmquistite is of interest, as non-stress conditions of development are indicated, in comparison with the monoclinic character of glaucophane, which he regards as a stress mineral. Ginzburg and Ginzburg (1950) record that there is no preferred orientation of the Kola holmquistite. In the Benson examples, however, there is a marked directional metamorphic texture with strong parallelism of the holmquistite crystals, suggesting that it may develop and persist under certain metamorphic conditions where stress is operative, as well as under static conditions, provided that Li is available.

Geochemical considerations.

The interesting observation by Ginzburg and Ginzburg (1950), that holmquistite forms at the expense of hornblende in the country rock with a simultaneous formation of clinozoisite at the expense of plagioclase, compares favourably with similar alteration processes of hornblende into cummingtonite, often observed in metamorphic rocks of dioritic and gabbroic composition. In both cases one of the major elements to be removed from hornblende is calcium, but the fixation of the liberated calcium ions is not always apparent.

It is possible that holmquistite has been formed in this way in most of the recorded instances, even when gradual changes have not been noticed, as in the present case, due to complete recrystallization. The fixation of calcium may be indicated by the presence of fluorite in the contact zones of the Benson occurrences, by apatite in the Kola finds, and by the remarkable formation of calcite between the holmquistite zone and the unaffected hornblendite rock in the Lacorne area. The

TABLE I. Chemical composition and atomic ratios to 24 (O,OH,F) of holmquistite and an associated hornblende from Mtoko, together with atomic ratios of holmquistites from other localities.

	1.	2.	1a.		3.	4.	5.	6.	2a.
SiO_2	59·06	44·06	Si	7·89 $Z = 8·00$	8·11	7·96 8·00	7·39 8·00	7·92 8·00	6·54 8·00
Al_2O_3... ...	12·38	12·84	Al... ...	0·11 1·84	1·15	0·04 2·03	0·61 1·69	0·08 1·67	1·46 0·78
TiO_2	0·20	0·97	Ti... ...	0·02 $Y = 2·10$	0·00 2·10	0·01 2·27	0·06 1·93	0·02 1·99	0·11 1·30
Fe_2O_3 ...	2·36	3·70	Fe''' ...	0·24	0·95	0·23	0·18	0·30	0·41
FeO	10·84	14·40	Fe'' ...	1·21	0·55	1·01	1·15	0·99	1·78
MnO	0·25	0·25	Mn ...	0·03 $X = 3·00$	0·05 2·98	0·02 2·93	— 3·01	0·02 3·02	0·03 3·74
MgO	8·82	8·74	Mg ...	1·76	2·38	1·90	1·86	2·01	1·93
CaO	0·21	11·04	Ca ...	0·03	0·01	0·15	0·19	0·08	1·76
Na_2O... ...	0·11	1·72	Na ...	0·03 $W = 1·86$	0·13 2·11	0·06 1·53	0·17 1·76	0·05 2·06	0·49 2·40
K_2O	0·05	0·31	K... ...	0·01	0·05	0·00	0·12	0·03	0·06
Li_2O	3·33	0·15	Li... ...	1·79	1·92	1·32	1·28	1·90	0·09
H_2O+ ...	2·09	1·81	OH ...	1·86	2·03	1·69	2·78	1·84	1·78
H_2O- ...	0·07	0·16	F	0·08 24	0·09 24	0·06 24	— 24	0·10 24	— 24
F	0·18	—	O	22·06	21·88	22·25	21·22	22·06	22·22
	99·95	100·15							
Less O for F ...	0·08								
	99·87								
			Sp. gr.	3·09	3·09	2·95	3·111	—	3·26
			α	1·624	1·640	1·624	1·625	1·622	1·655
			β	1·644	—	1·645	1·645	1·646	—
			γ	1·651	1·663	1·651	1·654	1·650	1·674
			$2V_\alpha$	52°±1°	44°	50°	51°	49°	76°
			γ:[001]	0°	0–2°	0–4°	0°	0°	19°

1. Holmquistite from Benson mine, Mtoko, Southern Rhodesia. Anal. O. von Knorring.

2. Hornblende (ass. with holmquistite from Benson mine). Anal. O. von Knorring.

1a. Atomic ratios of holmquistite from Benson mine to 24 (O,OH,F).

3. Atomic ratios of holmquistite from Utö, Sweden. Anal. A. Bygdén.

4. Atomic ratios of holmquistite from the Kola peninsula. Anal. A. M. Bondareva.

5. Atomic ratios of holmquistite from Alexander Co., North Carolina. Anal. E. V. Shannon.

6. Atomic ratios of holmquistite from Lacorne area, Quebec Province. Anal. J. A. Maxwell.

2a. Atomic ratios of hornblende from Benson mine, Mtoko, Southern Rhodesia.

chemical data of holmquistite and the coexisting hornblende from Benson mines are given in table I, together with atomic ratios of holmquistites from other described localities. A qualitative spectrographic analysis by Miss J. M. Rooke showed in addition traces of V, Cr, and Ni in the present holmquistite.

A comparison of the holmquistite analyses from the recorded occurrences shows very similar values for the *Y* and *X* groups, approximately 2 and 3 respectively, indicating a close agreement with the holmquistite formula Li_2 (Mg, Fe)$_3$ (Al, Fe)$_2$ Si_8O_{22} (OH, F)$_2$ as proposed by Ginzburg *et al.* (1958). It moreover appears from the above data that the major changes in the chemical composition are confined to these two ionic groups. The compositional variations are perhaps mainly controlled by the chemistry of the host rock, and to a certain extent by the nature of the metasomatic agents and the distance from the pegmatite contact. A unique example is the holmquistite from Kola containing CO_2 in the form of gas and liquid inclusions. In the present occurrence fluorine may have played an important role in the transfer of lithium during metasomatism. This is indicated by the abundance of fluorine-bearing minerals developed at the contact, and indeed an excess of fluorine and other volatiles in addition to lithium may be essential for the formation of a mineral like holmquistite in the country rock. The associated hornblende shows similar chemical features and carries also a small amount of lithium. Sundius (1947) recorded a hedenbergite pyroxene containing approximately 0·5 % lithium as an associate of the holmquistite from Utö.

References.

[Ginzburg (A. I.) and Ginzburg (I. V.)] Гинзбург (А.И.) и Гинзбург (И.В.), 1950. Доклады Акад. Наук СССР [Compt. Rend. Acad. Sci. URSS], vol. 74, p. 1119.

[Ginzburg (I. V.), Rogachev (D. L.), and Bondareva (A. M.)] Гинзбург (И. В.), Рогачев (Д. Л.), и Бондарева (А. М.), 1958. Ibid., vol. 119, p. 1013 [M.A. **14**–138].

Karpoff (B.), 1960. Rept. 21st Internat. Geol. Congr., Pt. 17, p. 7.

Machatschki (F.), 1953. Spezielle Mineralogie. Wien (Springer).

Osann (A.), 1913. [Sitzungsber. Heidelberger Akad. Wiss., Abh. 23]; quoted in Min. Mag., vol. 17, p. 352.

Palache (C.), Davidson (S. C.), and Goranson (E. A.), 1930. Amer. Min., vol. 15, p. 280 [M.A. **4**–526].

Sundius (N.), 1946. Årsbok Sveriges Geol. Undersök., vol. 40, no. 4 (Avh. Upps., Ser. C, no. 480) [M.A. **10**–70].

—— 1947. Geol. Fören. Förh., vol. 69, p. 51.

—— 1959. Amer. Min., vol. 44, p. 669.

Vogt (T.), Bastiansen (O.), and Skancke (P.), 1958. Ibid., vol. 43, p. 981.

SHORT COMMUNICATIONS

Juddite from Kajlidongri manganese mine, Jhabua District, Madhya Pradesh, India.

While studying the minerals from the Kajlidongri mine, I came across a red amphibole showing remarkable pleochroism and optical characters. The mineral occurs as small prisms, usually 2 to 3 mm. long, and is red in colour. The manganese ore associated with the mineral is of a striking reddish colour. Under the microscope the mineral is seen to occur as small prisms in a medium-grained quartzite showing a slight schistose texture. Where it occurs with the manganese ore the mineral is usually associated with blanfordite, calcite, and biotite.

The optical characters of the mineral are as follows: α 1·659, γ 1·681, γ–α 0·022, $2V_\gamma$ 66° to 72°, α:[001] 21° to 33°, elongation negative; pleochroism: α light carmine to deep carmine, β colourless to pale blue with a tinge of violet, γ light pinkish orange to orange with sometimes a tinge of brown, $\alpha > \beta > \gamma$. There is, however, great variation in the pleochroism. In some cases it is zonal with the stronger colour in the central part.

The optical characters of the mineral under study are very similar to those of the amphibole juddite described by the late Sir Lewis Fermor[1] who first described it from Kacharwahi in the Nagpur District. Fermor noted the remarkable pleochroism of the amphibole and named it in honour of Prof. J. W. Judd, as a tribute from a former student. Bilgrami[2] has also reported juddite from the Chikla mine, Bhandara District, Maharastra State, and has given its optical properties and chemical analysis. Recently Zwaan and Van Der Plas[3] described the optical and X-ray properties of juddite from the Nagpur District. The optical characters of the amphibole, such as negative elongation, positive optic axial angle, and refractive indices suggest that it is closely related to the alkali amphiboles, especially to the riebeckite group as described by Miyashiro.[4]

This work was carried out at the Laboratory of Applied Geology,

[1] L. L. Fermor, Mem. Geol. Surv. India, 1909, vol. 37, pt. 1, p. 159.

[2] S. A. Bilgrami, Min. Mag., 1955, vol. 30, p. 636.

[3] P. C. Zwaan and L. van der Plas, Konink. Nederl. Akad. Wetensch., ser. B, 1958, vol. 61, p. 266.

[4] A. Miyashiro, Journ. Fac. Sci. Univ. Tokyo, Sect. II, 1957, vol. 11, p. 57.

Saugar University. I am grateful to Prof. W. D. West for critically going through the paper.

Dept. of Applied Geology,
University of Saugar,
Saugar, (M.P.), India.

V. K. Nayak

The identity of namaqualite with cyanotrichite.

In 1870 (Jour. Chem. Soc., vol. 23, p. 1) Professor A. H. Church described as a new mineral, namaqualite, some material obtained by J. R. Gregory, who brought it from Namaqualand in South Africa. Church's description is as follows:

> . . . Namaqualite occurs in thin layers of silky fibres which are true crystals, though their minute size and general absence of distinct terminations renders it impossible to ascertain the system to which they belong. The layers alternate with irregular bands of a kind of chrysocolla, and are sparingly mixed with small crystals of magnesia mica. The aspect of namaqualite resembles that of chrysolite [i.e. *chrysotile*], but its colour is pale blue with a silky lustre. Its hardness is 2·5, and its density 2·49. Isolated crystals appear transparent under the microscope. In the closed tube it gives off much water when heated, becoming black.
>
> For analysis, the mineral was coarsely crushed, and the homogeneous fragments carefully picked out under the microscope. . . . The mean percentages are: H_2O 32·38, CuO 44·74, Al_2O_3 15·29, CaO 2·01, MgO 3·42, SiO_2 2·25, Sum 100·09.

Church therefore considered it a hydrated copper aluminium oxide, and suggested a possible relationship to hydrotalcite and pyroaurite. Apparently no further investigation has been reported in the literature since Church's original paper.

In the mineral collection of the American Museum of Natural History there is a single specimen (no. 6176) labelled 'Namaqualite, Namaqualand, South Africa', which agrees with the description given by Church. It was purchased from J. R. Gregory, and is probably part of the same material he supplied to Church. In immersion liquids under the microscope the blue mineral appears as aggregates of fibrous crystals, strongly pleochroic from almost colourless to bright blue, and with α 1·59, γ 1·65; these properties are identical with those of cyanotrichite, and the identity was confirmed by the comparison of an X-ray powder photograph with that of a specimen of cyanotrichite from Moldawa, Rumania. The analysis given by Church evidently reports as H_2O the loss in ignition, which would include the SO_3 also present in cyanotrichite. The formula of cyanotrichite requires 12·4 % SO_3 and 22·4 % H_2O, their

sum being in reasonable agreement with the figure of 32·4 % 'H_2O' reported by Church. His figures for CuO and Al_2O_3 agree well with those for cyanotrichite.

In the 7th edition of Dana's System of Mineralogy, Professor Frondel reports cyanotrichite from the Springbok Mine, Namaqualand. Professor Frondel informs me that this specimen was presented to Harvard University by the late Dr. P. Wagner in 1927, and the identification on the original label was 'namaqualite?' It is quite possible that this is the locality from which the original specimens of namaqualite were obtained.

American Museum of Natural History,
New York.

Brian Mason

Aluminium laps for polished sections.

An outstanding difficulty in the use of diamond powders is the plucking of fractured grains of chalcopyrite, &c. Cloths are useful, but cause too much relief for general purposes. Solid nylon is slow, while solid metal laps such as copper still cause injury to fractured sulphide ores though useful with rocks.

Lead laps have been used successfully, but are expensive and liable to alteration. In the hope of combining the soft action of cloth with the diamond-holding property of the metal the writer has tried copper gauze without success. Recently a soft aluminium foil has been available in household stores. This is very thin and flexible and was found to accept the diamond powders in the same way as lead. Accordingly it was attached to glass discs to form a smooth metal surface which provided a level polishing lap, but the surface was still very rigid, like that of the solid metal laps. By chance it was found convenient to attach the foil by an intermediate sheet of thin paper, and this caused a great improvement in the action of the lap, which gave sharp cross-cutting with very little relief, yet the cushioning effect of the paper support greatly reduced the damaging effects of contact with the metal. The surface so produced is not level in the optical sense, but local differences between neighbouring grains are very small; a little relief is introduced by the usual finishing polish with alumina, &c., on selvyt cloth.

A very convenient aluminium foil lap can be made from a special thin foil, which is already attached to a paper back. This is sold by dealers in packaging materials. The paper side is smoothly mounted on a glass disc with Seccotine. A small drop of 5Cs silicone (Hallimond, Manual

of the Polarizing Microscope) with diamond powder is placed on the lap and the running time is usually about 5 minutes; speed about 100 r.p.m. for a 6-inch lap with triple holder; weight 2/3 lb.per 1-inch mount. The lap is cleaned with methylated spirit. Several runs may be needed to remove earlier cavities. The diamond should not be coarser than 3 μ, after which a final cutting stage is provided by 1 μ. Quartz is now polished, but softer minerals require a brief hand polishing with magnesia, alumina, or $\frac{1}{4}$ μ diamond on selvyt. In spite of the small thickness the laps have a satisfactory life and are very cheap.

75 *Corringham Road,*
London, N.W. 11.

A. F. Hallimond

BOOK REVIEWS

Tolansky (S.). *Surface Microtopography.* London (Longmans, Green & Co. Ltd.), 1960. viii+296 pp. Price 55*s*.

This book gives an account of interferometric work, mainly multiple-beam interferometry, carried out in the author's laboratories. The principles, methods, and apparatus are described fairly briefly and the major part of the book is devoted to varied applications. The latter cover a wide field of pure and applied science. Very detailed studies have been made of the topography of faces of naturally occurring crystals of diamond and quartz, and of synthetic quartz and silicon carbide. These yield fascinating evidence of the mode of growth of such crystals. Much interesting work has been done on the cleavage of minerals, including the opposite surfaces of one cleavage plane. Etching of crystal faces and cleavages are also described. The later part of the book is devoted to studies of the vibrations of quartz oscillator plates, indentation hardness testing of metals, the directional hardness and abrasion of diamond, and other topics. The text, together with the 359 photographs that are reproduced, illustrate the power of interferometry for very refined measurement on nearly plane surfaces. It is possible, in special circumstances, to measure steps of a few Ångstroms, and in one case the steps of a growth spiral were found to have a height of only 2·3 Å.

The merits of this book are marred by a number of unnecessary inaccuracies, the text is not always lucid, and crystallographic presentation is weak. In some cases one would draw different conclusions from the evidence presented. A. F. S.

SMALES (A. A.) and WAGER (L. R.), editors. *Methods in Geochemistry.* Interscience Publishers Ltd. (New York and London), 1960, viii and 464 pp., 103 figs. Price 94*s*.

During the last decade an enormous amount of geochemical research has been carried out and one of the main reasons for this has undoubtedly been the increasing and successful application of new laboratory techniques to geochemical problems.

The results of these investigations, but not necessarily the methods, have been published in a large number of journals all over the world, and the editors of the book under review have now decided to present these methods together with examples of their use, in one volume. The plan of the editors has been to invite specialists to write readable and informative accounts of particular techniques, and the book is, therefore, divided into eleven chapters, chapter 1 (written by the editors) being an introduction. The authors and titles of the remaining chapters are: 2, L. R. Wager and G. M. Brown, 'Collection and Preparation of Material for Analysis'; 3, E. A. Vincent, 'Analysis by Gravimetric and Volumetric Methods, Flame Photometry, Colorimetry and Related Techniques'; 4, S. R. Taylor and L. H. Ahrens, 'Spectrochemical Analysis'; 5, H. I. Shalgosky, 'Fluorescent X-ray Spectrography'; 6, K. I. Mayne, 'Stable Isotope Geochemistry and Mass Spectrometric Analysis'; 7, R. K. Webster, 'Mass Spectrometric Isotope Dilution Analysis'; 8, S. Moorbath, 'Radiochemical Methods'; 9, D. Mapper, 'Radioactivation Analysis'; 10, S. Moorbath, 'Polarography'; 11, F. W. Cornish, 'Some Modern Chemical Separation Methods'.

The authors of chapters 2, 3, 4, 5, 10, and 11 have had the advantage of writing on subjects that are to a large degree complete in themselves, and they have carried out their task well enough, although parts of chapter 2, and in particular the section on the preparation of meteorites for analysis, are dealt with too briefly. The substance of chapters 6, 7, 8, and 9 on the other hand overlap to some extent and in an effort to preserve conciseness and lucidity there have been some lapses, possibly editorial. The same matter is explained in more than one chapter, not always equally efficiently, and instances can be found where the author has assumed that the reader has prior knowledge of the subject. Thus, in chapter 6, page 157, figure 1 is incomplete and the text gives no help in understanding it, and on page 176 the formation of ^{3}He by the reaction $^{14}N\ (n,\ 3\alpha)^{3}H$ is not obvious. Occasionally, also, the reader encounters such terms as 'spike' and 'hold back carrier': these terms merit a few words in explanation. These four chapters are probably the

most important in the book and it might well have served the editors' purpose better if the authors had been asked to collaborate. In chapter 11, where the methods of separation discussed are those of ion exchange, solvent extraction, and paper chromatography, the reader may think that too much space has been devoted to theoretical considerations. The chapters are supplemented by copious references, which, except for those at the ends of chapters 6, 8, and 10, are arranged alphabetically.

Apart from these criticisms there can be no doubt that the editors have succeeded in presenting a concise and informative account of modern analytical methods in geochemistry and the book can be recommended unreservedly. A. A. M.

DE JONG (W. F.). *Kompendium der Kristallkunde.* Wien (Springer-Verlag), 1959. 258 pp., 227 text-figs. Price $10.50 or 75*s*.

—— *General Crystallography: A Brief Compendium.* London (W. H. Freeman & Co., Ltd.), 1960. x+281 pp., 231 text-figs. Price 38*s*.

These two books are independent translations, with some revision and rewriting, of the original Dutch edition of 1951.

They provide a clearly written, highly condensed account of modern crystallography in its proper setting as a department of physics. The author does not hesitate to go into the details of mathematical explanation where necessary, and thus provides data that are not to be found in many more voluminous textbooks. The book is sub-divided into four main parts: 'Geometric Crystallography', 'Crystal Structures', 'Crystal Chemistry', and 'Crystal Physics'.

The first part is the most extensive and gives a clear survey of the basic laws of geometrical crystallography, as well as symmetry elements and their derivation. After some aspects of direct and indirect lattices, different methods of calculating angles are discussed. Fourteen pages are devoted to different methods of crystal projection, the main emphasis being laid on the stereographic projection. The discussion of its practical application is a welcome addition.

A prominent feature of the second part is the mathematical interpretation of the refraction of X-rays in the crystal structure. All the important methods used for structural determination are briefly mentioned and illustrated with most informative diagrams. There are few textbooks of this size that give as de Jong does a clear survey of Weissenberg and retigraph methods, and enter into the mathematical background of Fourier analysis and Patterson synthesis.

The third section of the book ('Crystal Chemistry') deals briefly with types of bond. Unfortunately, important features, as for instance isomorphism and isotypism, are treated extremely briefly. The most important lattice types, both organic and inorganic, are clearly illustrated and provide an excellent survey for the student.

Remarkable is the sub-division of 'Crystal Physics' into a descriptive and an explanatory part. Mechanical, optical, electrical, and magnetic characteristics of crystals are summarized in the first chapter. The author lays much emphasis on tensor mechanics as applied to crystal physics. He stresses the importance of problems of elasticity and deformation and his treatment suggests that the dominant position taken by crystal optics in many textbooks is not entirely justified. Nevertheless the main features of crystal optics are dealt with in a comprehensive and clear way, assisted by excellent diagrams. The definitions are simple and straightforward. Cleavage, hardness, diffusion, Frenkel and Schottky defects, resonance, and crystal growth, as well as some practical applications (transistors, detectors, &c.), are discussed in the second chapter.

The reader, whether or not mathematically inclined, will find the book a concise yet comprehensive account of modern crystallography.

E. F. Stumpfl

Mason (Brian H.). *Trap Rock Minerals of New Jersey.* New Jersey Geological Survey, Department of Conservation and Economic Development. Bulletin 64, 1960, 51 pp., 16 figs., 1 map. $1.50.

This booklet gives an interesting and up-to-date account of the minerals of the trap rocks of New Jersey with special reference to the zeolites. A description of the occurrence and paragenesis is followed by some details of the localities. The species (of which there are sixty) are arranged in systematic order. Each mineral has a section devoted to its basic properties, followed by a note on the occurrence in New Jersey. Although it is not specifically stated, the general information on each mineral (which would be found in any elementary textbook) and the notes on the zeolite group suggest that the book is primarily for the amateur. It is very well illustrated from specimens in the American Museum of Natural History and has a useful map and bibliography. An unusual and helpful addition is a list of discredited and unconfirmed occurrences, but there is no general index.

J. M. S.

Davies (G. M.). *A French–English Vocabulary in Geology and Physical Geography* (reprint of 1st edition (1932)). John Mann. Pp. 140+ix. Price 18*s*.

This glossary of some 5,000 terms, being a reprint of the first (1932) edition, is to some extent out of date. Allowing for this, it gives a reasonably comprehensive vocabulary in physical geography and general geology. In stratigraphy it is more than comprehensive, many terms familiar in English geological literature with the same usage as in French being included both in the list and in the stratigraphical tables (Appendix I). It is, however, less complete and accurate in mineralogy and petrology in which the author's policy of extreme brevity has led him to give definitions which are sometimes misleading and occasionally quite inaccurate. For example, gieseckite and gigantolite are described as varieties of nepheline and cordierite respectively, whereas they are pinite pseudomorphs after those minerals. In French, as in English, it may be difficult to decide what the usage of a rock name really is, and it is usual to quote an authority for it; nevertheless no such references are given. They would be particularly useful in support of definitions such as 'gneiss without mica' for leptynite and 'zircon-syenite' for miascite. There are also notable omissions in this field: e.g. the abbreviations N_p, N_m, and N_g for α, β, and γ, although many abbreviations in the general field are quoted (e.g. A to G for major subdivisions of the Lower Palaeozoic) that are internationally current. One last, perhaps unfair, criticism is that the price is rather high for a book of this size and scope.

S. E. E.

Gleason (Sterling). *Ultraviolet Guide to Minerals. A Complete Working Manual for the Use of Ultraviolet Light in Locating and Recognizing Minerals including Field Identification Charts.* Princeton, New Jersey; New York, Toronto, London (D. Van Nostrand Company, Inc.), 1960. 244 pp., 9 figs., 16 col. pls. with 61 figs. Price $6.95, 52*s*. 6*d*.

This is a book that will satisfy a long-felt want in an age in which the study of the fluorescence of minerals has become fashionable. As the preface claims, it is written to suit all types of readers. Introductory chapters dealing with fluorescent properties and use of ultraviolet lamps in the field are followed by useful charts to aid the identification of minerals by the colour of their fluorescence. Chapter VI deals with grading of gemstones by this method and chapter VII gives an

alphabetical list of minerals with localities and details of their fluorescence and phosphorescence under short-wave and long-wave ultraviolet light. Sections are also devoted to radioactive minerals, the uses of fluorescence in industry and mineral testing, and a résumé of its history and probable future. The book is illustrated by a number of coloured plates and has an adequate index. JESSIE M. SWEET

KUKUK (Paul). *Geologie, Mineralogie und Lagerstättenlehre.* Berlin (Springer Verlag), 1960. 354 pp., 433 figs. Price 28.50 DM.

This book is meant as an introduction to geology, mineralogy, and economic geology for students of mining schools and others who need the above-mentioned sciences as ancillary subjects. Special emphasis is put on practical aspects with regard to coal mining.

The first part (Geology) is subdivided into two main chapters: General Geology (105 pp.) deals briefly with the main rock types, some principles of structural geology, and a survey of exogenic and endogenic forces. For the sake of brevity, aspects of microscopic investigation of thin sections are omitted. Forty excellent drawings and photographs illustrate the survey of structural features. In stratigraphy the space devoted to the kainozoic period (considerably more than to the mesozoic) seems slightly exaggerated.

In the second part (Mineralogy) general aspects cover 20 pp., the systematic discussion of minerals 60 pp. The whole approach in the chapter on general mineralogy seems to be based on the old descriptive outlook and no justice is done to the fundamental facts of modern crystallography. The terminology, too, is often unsuitable or even incorrect. The systematic survey of minerals, arranged according to chemical principles, is a most welcome account. It is illustrated by 68 excellent photographs and drawings, which many more specialized textbooks do not provide in such quality and quantity. Physical properties, occurrence, and use of minerals are discussed. Many data of production and prices are given. A special feature, which even the more experienced geologist will appreciate, is that most mineral names are explained etymologically.

The third part of the book (pp. 240–340) deals with economic geology. Aspects of systematic subdivision are briefly mentioned and the importance of geophysical methods for prospecting is underlined. The systematic discussion of deposits is confined to those of Germany. The author devotes special interest to the Ruhr coal mining area (40 pp.) and some space to ore, salt, oil, and gas deposits. E. F. S.